

超音波影像實驗室

Ultrasonic Imaging Laboratory

Dr. Pai-Chi Li (李百祺博士)

Room 303
Department of Electrical Engineering
National Taiwan University
No.1, Sec.4, Roosevelt Road
Taipei, Taiwan 106, R.O.C.
TEL: + 886-2-23635251-303
[Http:// land.ee.ntu.edu.tw](http://land.ee.ntu.edu.tw)

Ultrasonic Imaging Laboratory Members

Advisor: Dr. Pai-Chi Li

Ph. D. Student: 4

Master Degree Student: 5

Administrators: 1

Research Assistant: 3

Graduated Student: 7 (M.S.)



Pai-Chi Li (Associate Professor, Senior Member of IEEE)
Electrical Engineering
National Taiwan University
+ 886-2-23635251-309
paichi@ee.ntu.edu.tw

PERSONAL EDUCATION

National Taiwan University	1983-1987	B.S.	Electrical Engineering
University of Michigan	1989-1990	M.S.	EE: Systems
University of Michigan	1991-1994	Ph.D.	EE: Systems

RESEARCH INTEREST

Signal and imaging processing, Ultrasonic medical imaging

WORK EXPERIENCE

Adjunct Associate Investigator	Health Research Institutes, Taiwan	2001-present.
Member of Technical Staff	Acuson Corporation, U.S.A.	1994-1997.

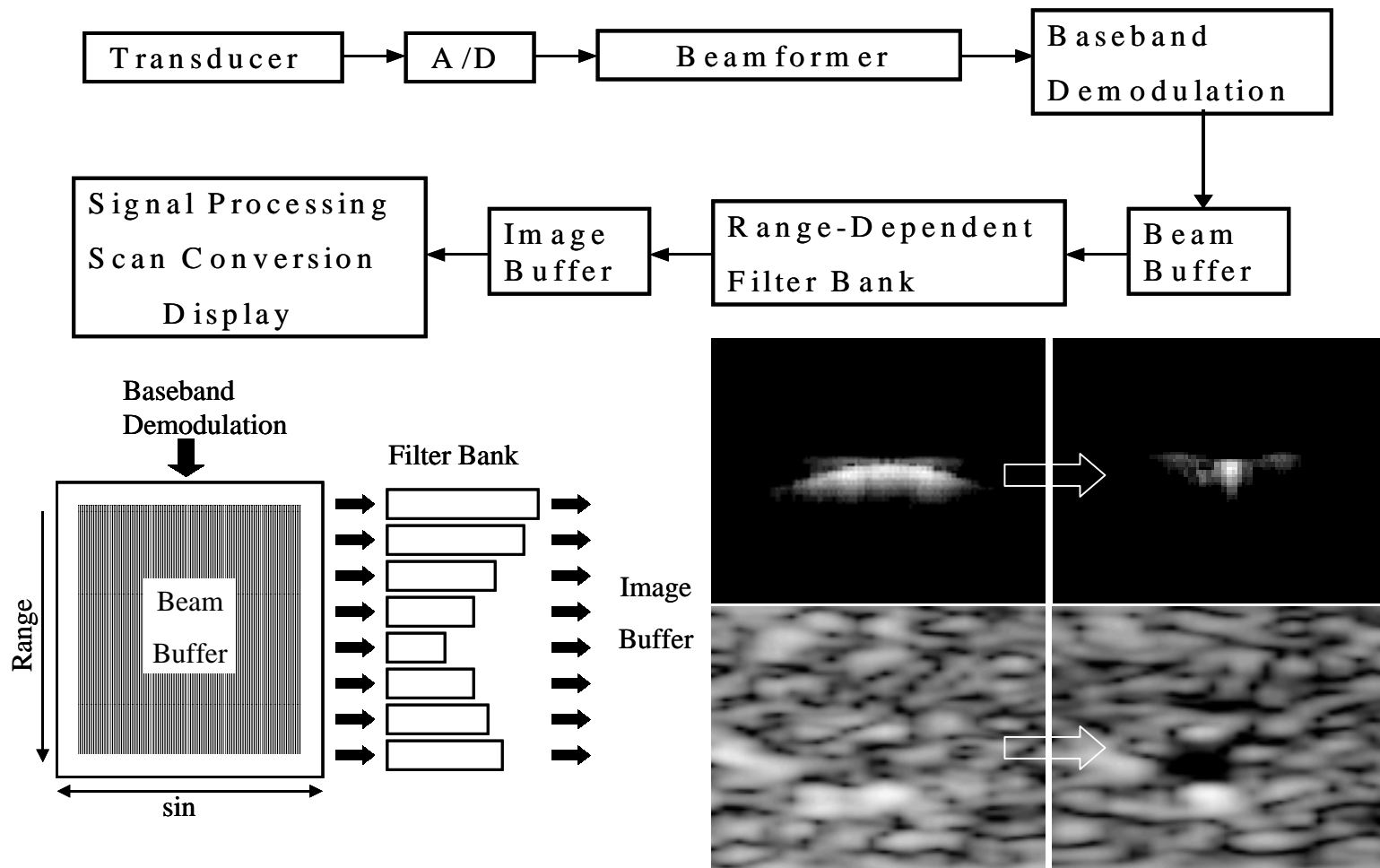
PROGRAM OVERVIEW

1. Ultrasonic Synthetic Aperture Imaging
and Adaptive Imaging
2. Ultrasonic Nonlinear Imaging
3. Ultrasonic Elastic Imaging
4. 3-D Ultrasonic Imaging
5. High Frequency Ultrasonic Imaging
6. Blood Flow Estimation Using Ultrasonic Contrast Agent

1. Ultrasonic Synthetic Aperture Imaging and Adaptive Imaging

• Ultrasonic Synthetic Aperture Imaging

– Filter based synthetic focusing technique

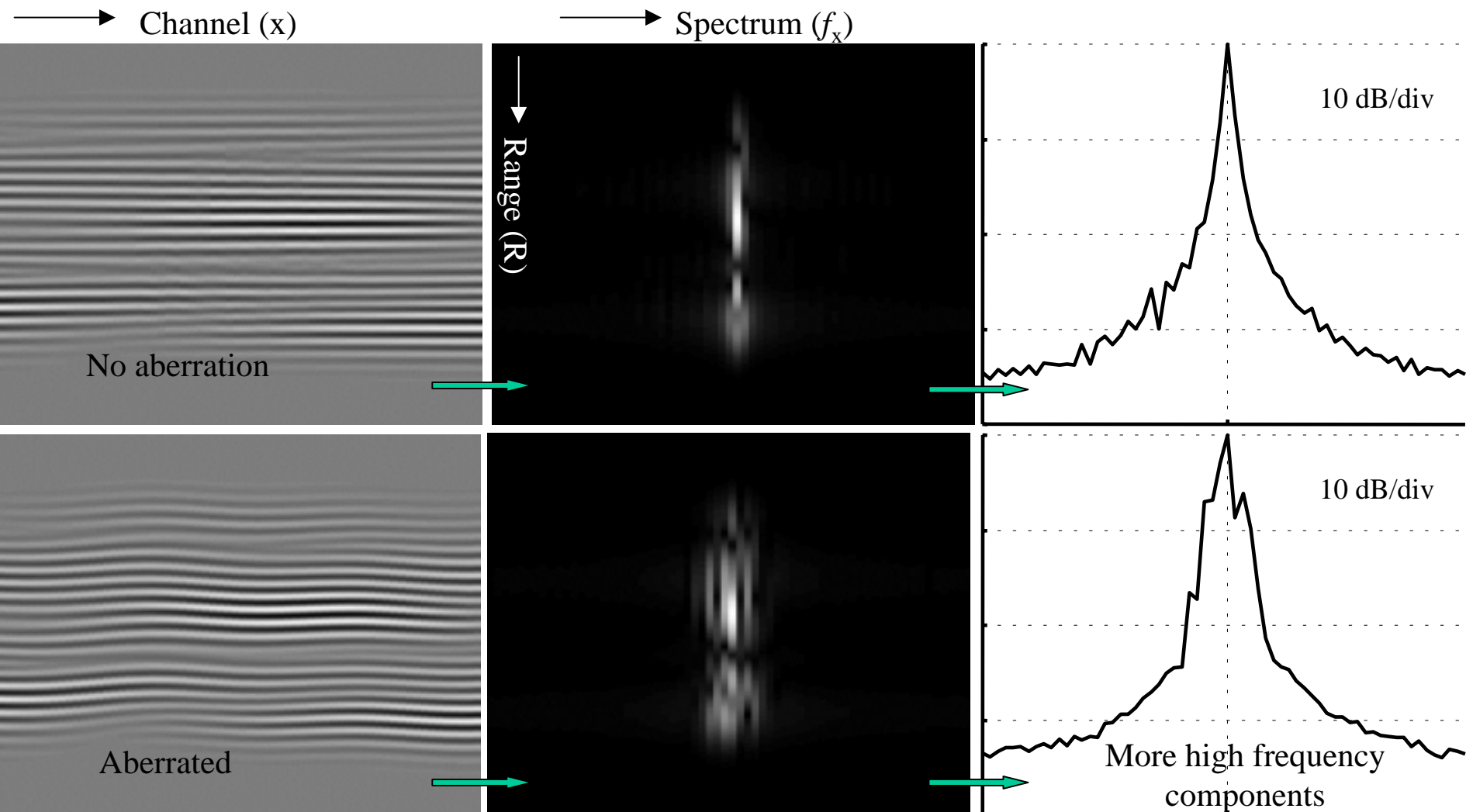


M.-L. Li and P.-C. Li, "Filter Based Synthetic Transmit and Receive Focusing", Ultrasonic Imaging, Vol. 23, pp. 73-89, April, 2001.

Adaptive Imaging

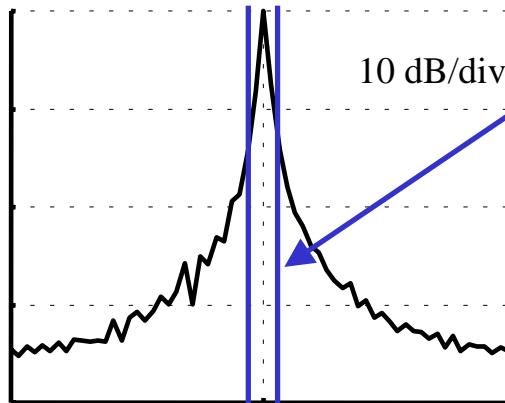
- A new adaptive imaging technique using generalized coherence factor (GCF) is proposed.
- GCF is derived based on the spectrum of the received array data along the array direction.
- GCF is an index of beamforming quality
- GCF is used as a weighting factor to the reconstructed image.

Idea



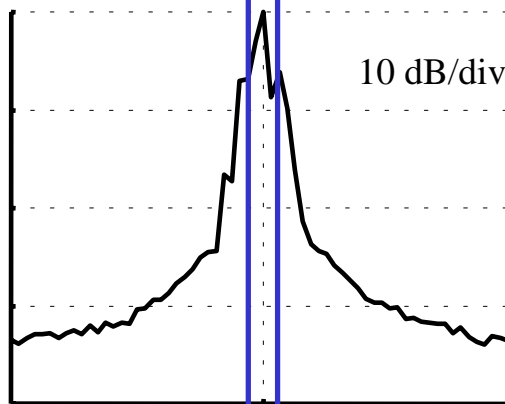
Generalized Coherence Factor

$$\text{GCF} = \frac{\text{spectral energy within a pre - specified low frequency range}}{\text{total spectral energy}}$$



No aberration

- High GCF corresponds to good focusing quality and the image intensity should be maintained



Aberrated

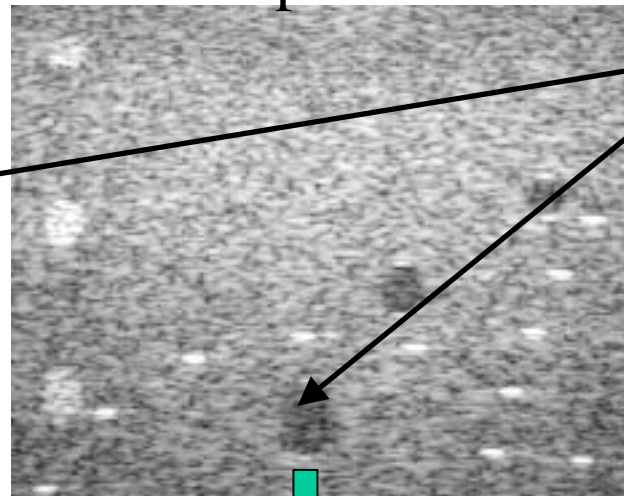
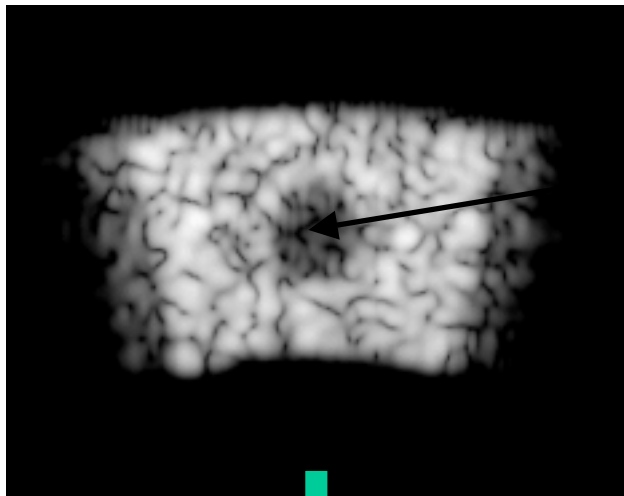
- Lower GCF should be used to reduce the image data because significant beamforming errors are present

Results

Simulation

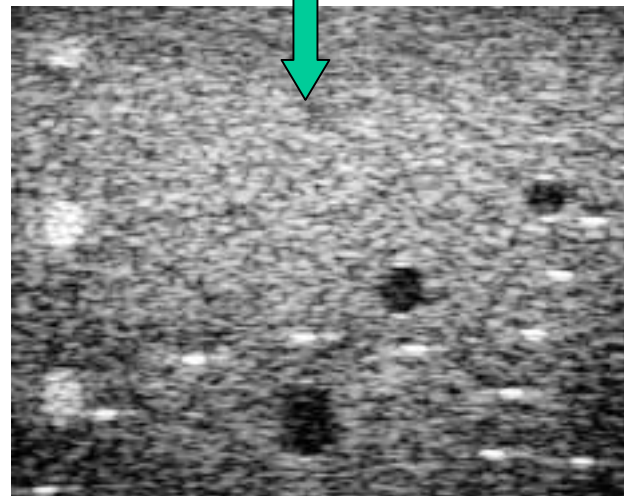
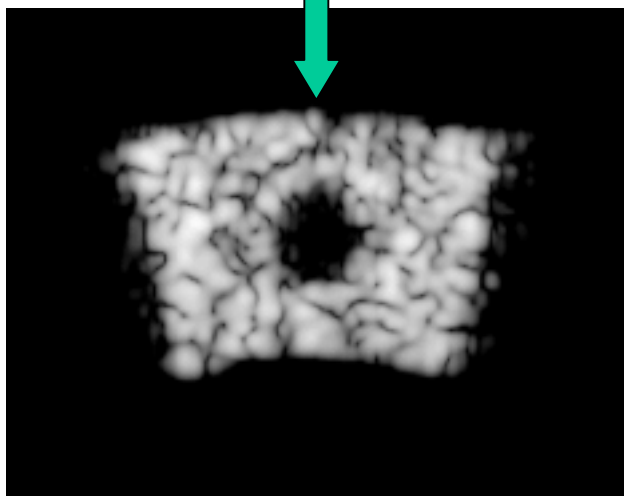
Experiment

Aberrated



Anechoic cyst

GCF Corrected

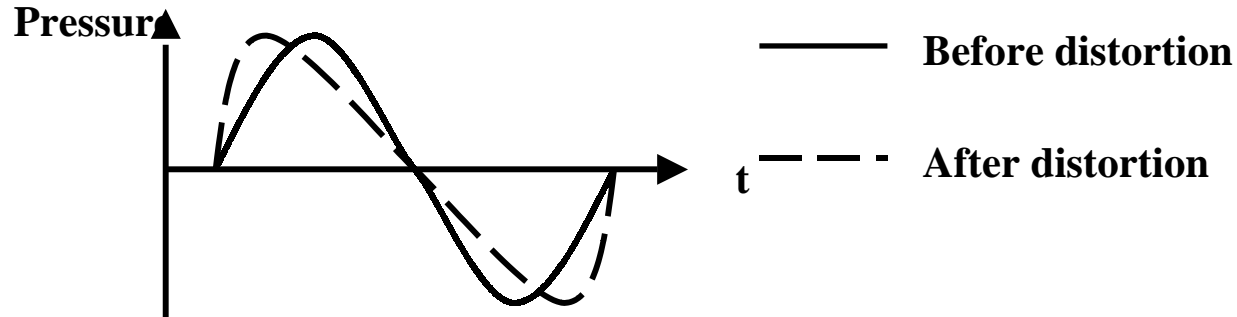


2. Ultrasonic Nonlinear Imaging

Ultrasonic Tissue Harmonic Imaging

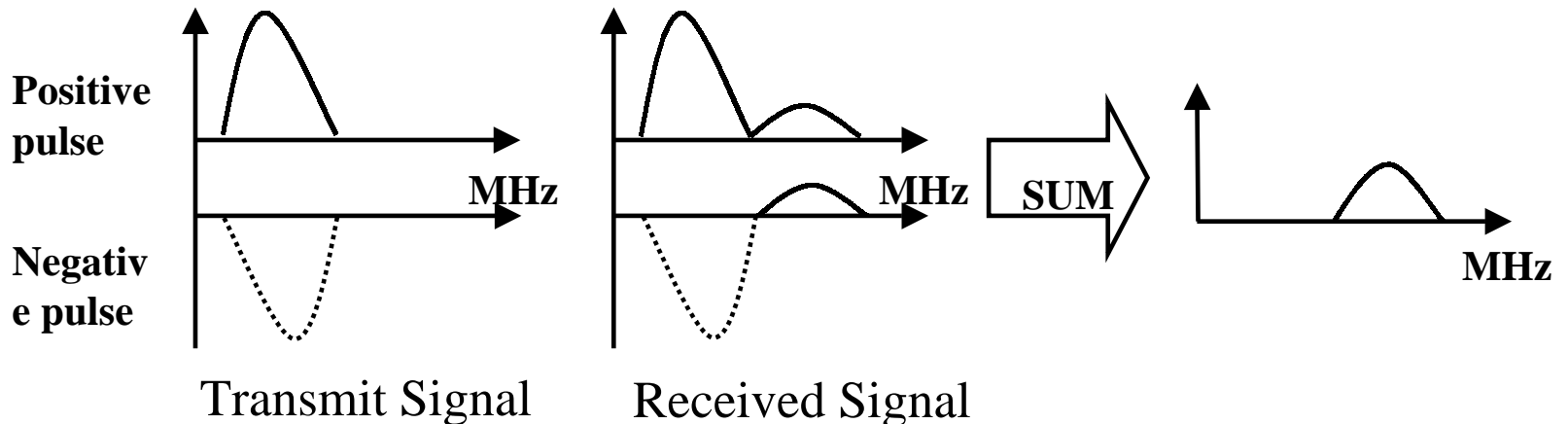
- **Tissue Harmonic**

- the harmonic component generated from *finite amplitude distortion*



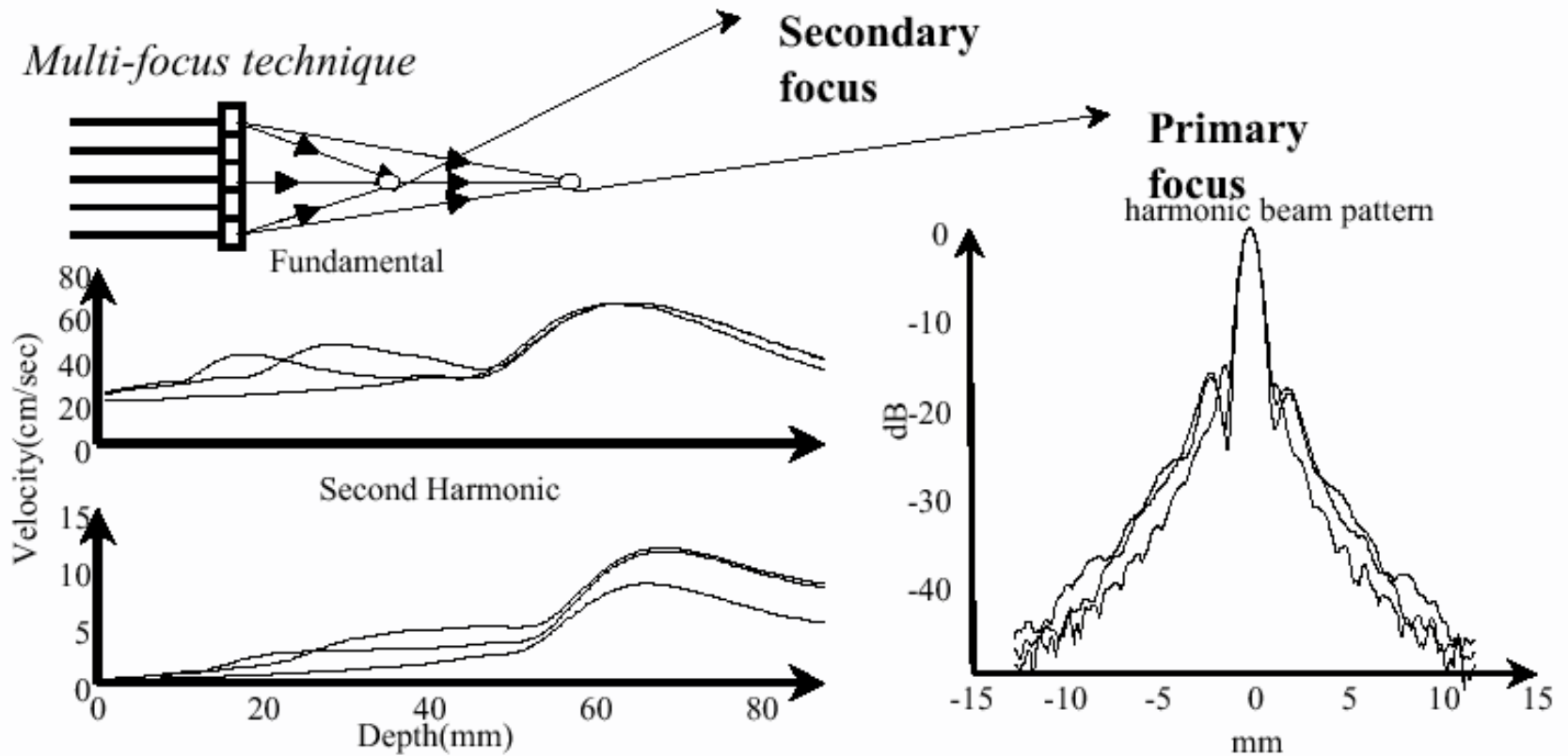
- **Pulse Inversion**

- Better fundamental rejection, lower frame rate



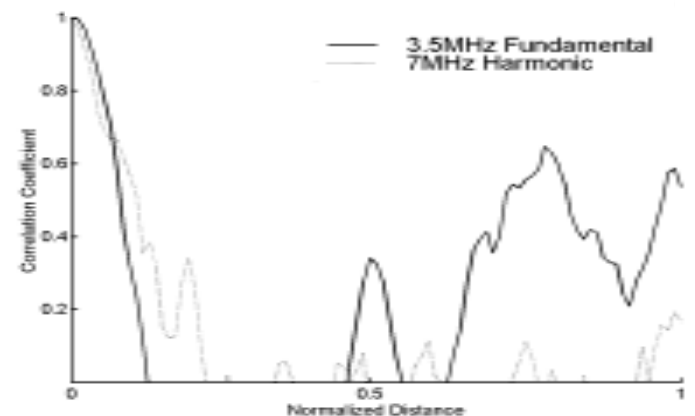
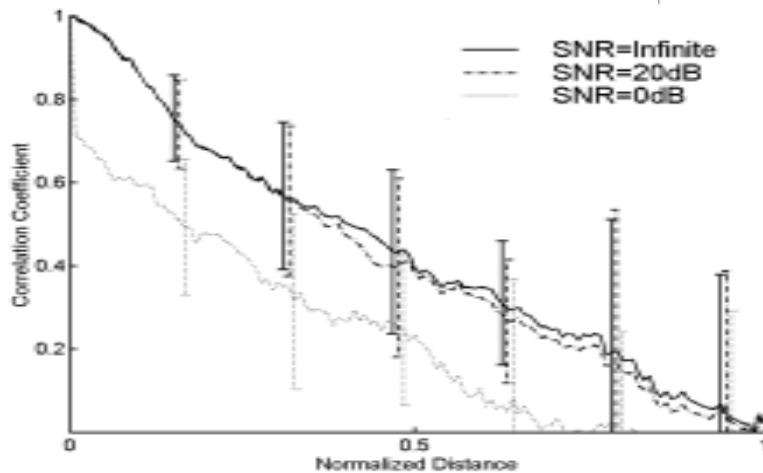
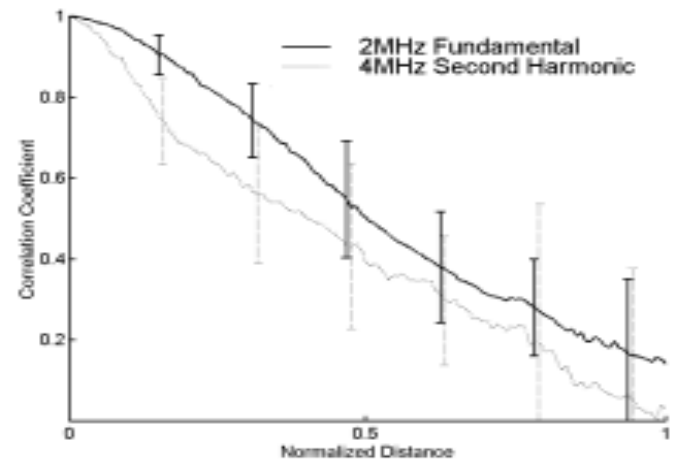
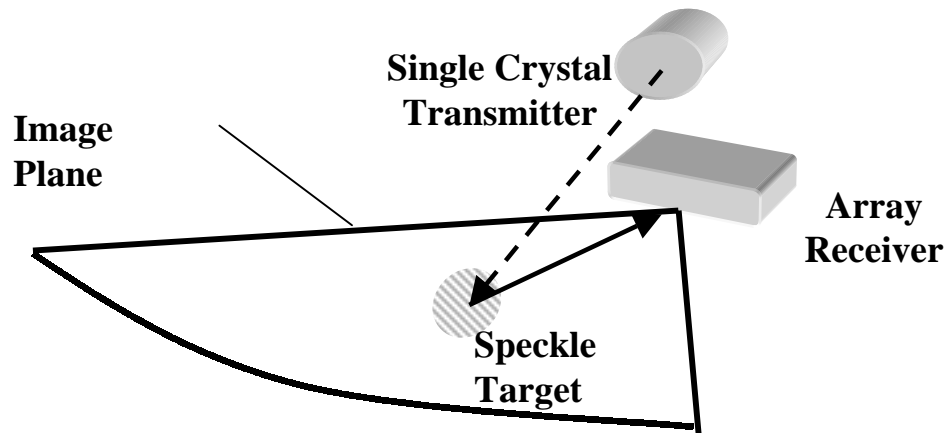
Ultrasonic Tissue Harmonic Imaging

- The Effect of Multi-focus Technique on Tissue Harmonic Image
- Effects of Harmonic Leakage on Tissue Harmonic Imaging



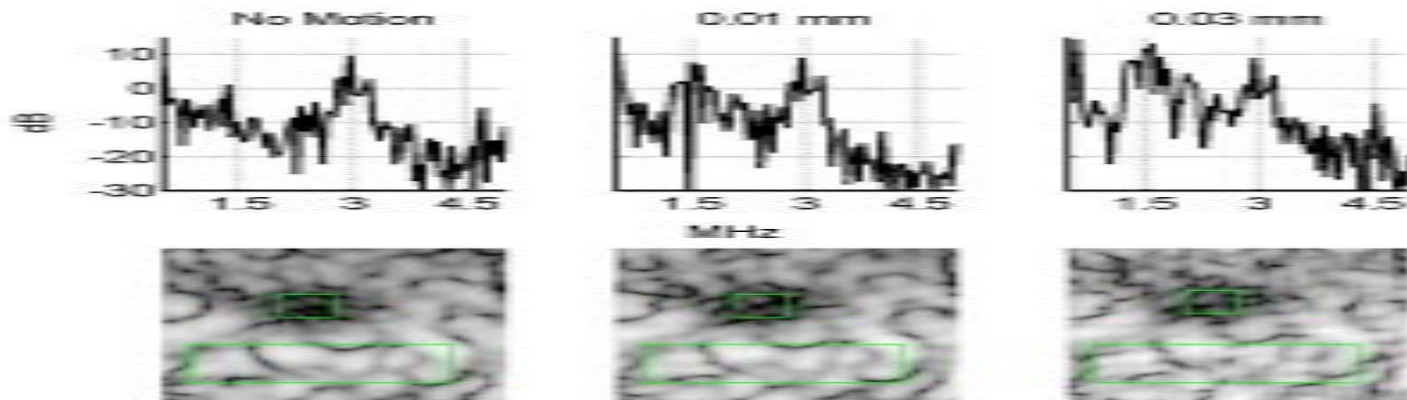
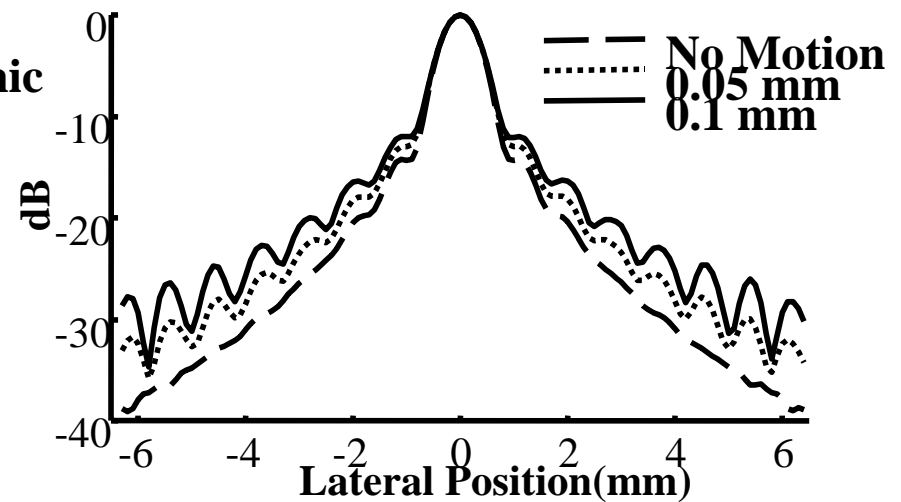
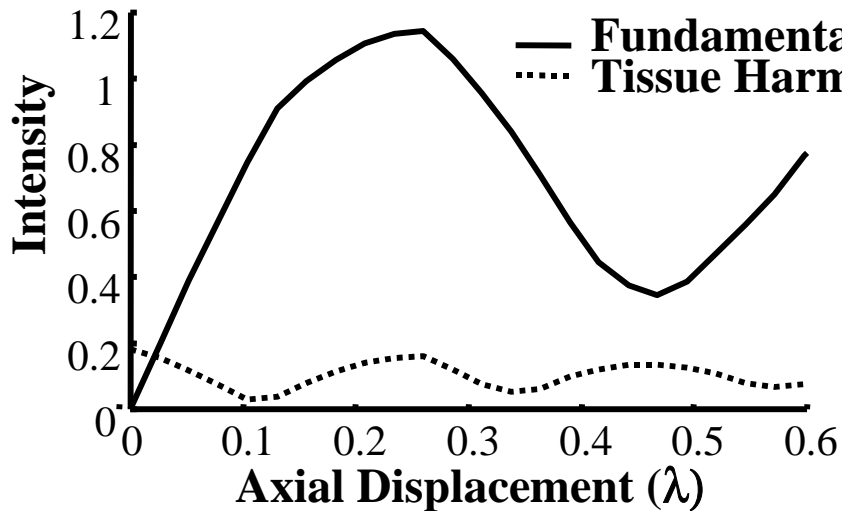
Ultrasonic Tissue Harmonic Imaging

- **Harmonic spatial covariance analysis**
 - Effects of SNR
 - Effects of sound velocity inhomogeneities



Ultrasonic Tissue Harmonic Imaging

- **Motion artifacts of Pulse Inversion Technique**
 - Effects of SNR
 - Effects of sound velocity inhomogeneities



3. Ultrasonic Elastic Imaging

Ultrasonic elastic imaging

- Ultrasonic strain compounding image based on a fast speckle tracking algorithm
- Strain compounding technique
 - Improve contrast resolution of the image
 - Steps:
 - Obtain an uncompressed image as a basis
 - Applying an external force on the object yields deformation
 - Modify the deformation in the image plane
 - Average the modified and original images

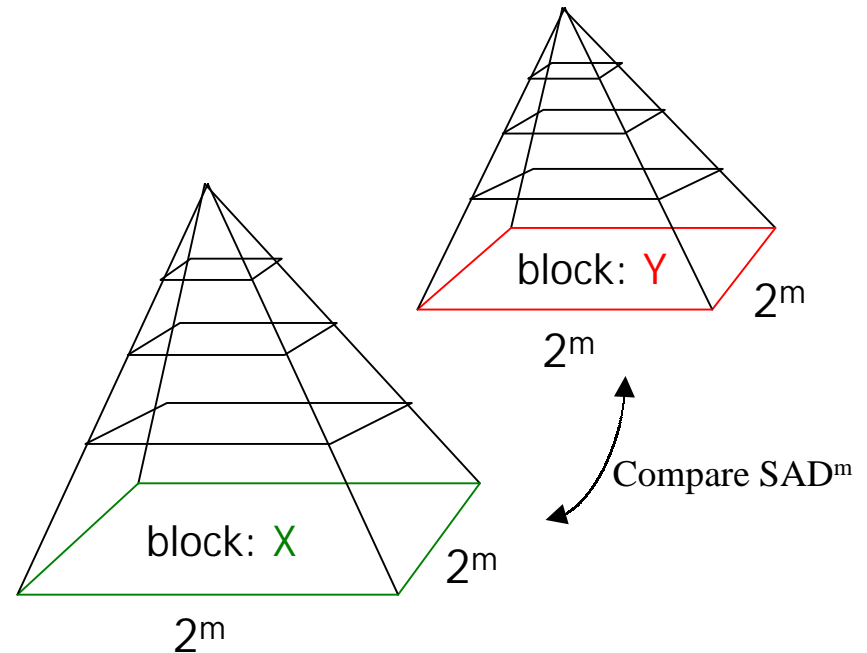
2D fast speckle tracking algorithm

- **Block Sum Pyramid**
 - Take threshold: SAD_{min}
 - Reduce the computations of SAD

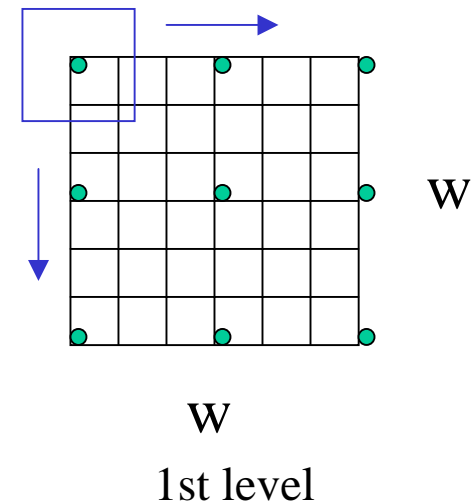
Pyramid structure

$$X^{m-1}(i, j) = X^m(2i-1, 2j-1) + X^m(2i-1, 2j) \\ + X^m(2i, 2j-1) + X^m(2i, 2j)$$

$$SAD^m(X, Y) = \sum_{i=1}^{2^m} \sum_{j=1}^{2^m} |X^m(i, j) - Y^m(i, j)|$$



- **Multilevel Block matching**
 - Reduce *numbers* of points to be searched
 - We use 2 levels
 - 1st level: window size = $w \times w$, 9 points
 - 2nd level: window size = $\frac{1}{2} \times w \times \frac{1}{2} \times w$, all points



Results

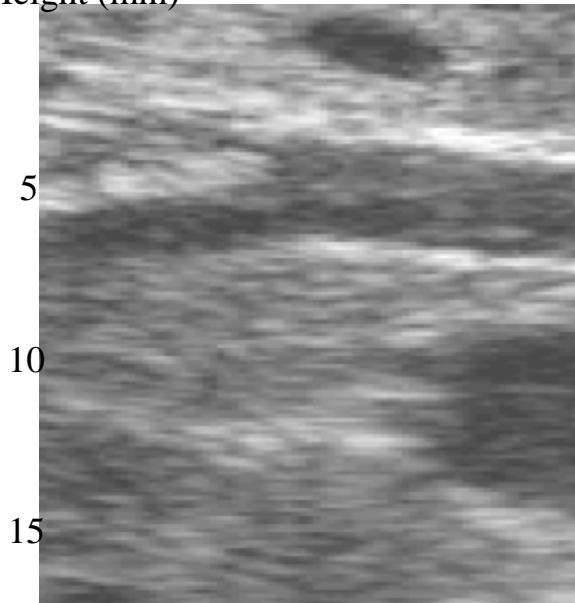
- Algorithm performance For 121 pixels

Language	FSA	BSPA	BSPA & Multilevel	Ratio
Matlab	27.14 (s)	14.17 (s)	7.64 (s)	3.6 : 2 : 1
C	12.3 (s)	1.53 (s)	0.998 (s)	12 : 1.5 : 1

BSP & Multilevel algorithm is indeed not only **faster** than traditional algorithm, but also as **accurate** as traditional one.

- Compounding image

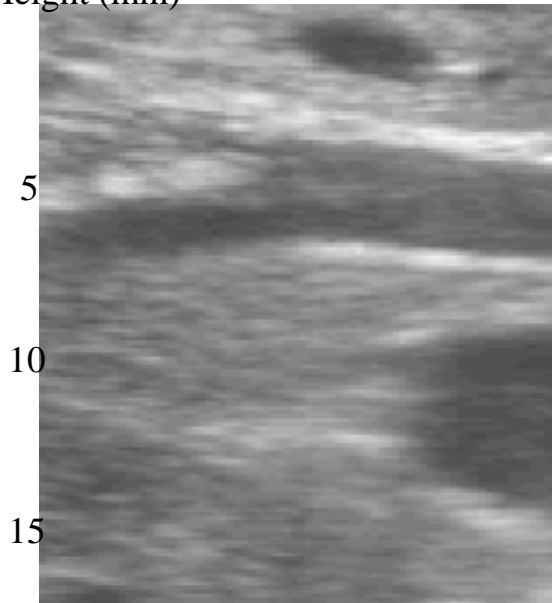
Height (mm)



Width⁵(mm)

L: original image

Height (mm)



Width⁵(mm)

R: compounding image with BSP & Multilevel

Liver

SNR=0.1164

SNR ↑

Computing speed ↑

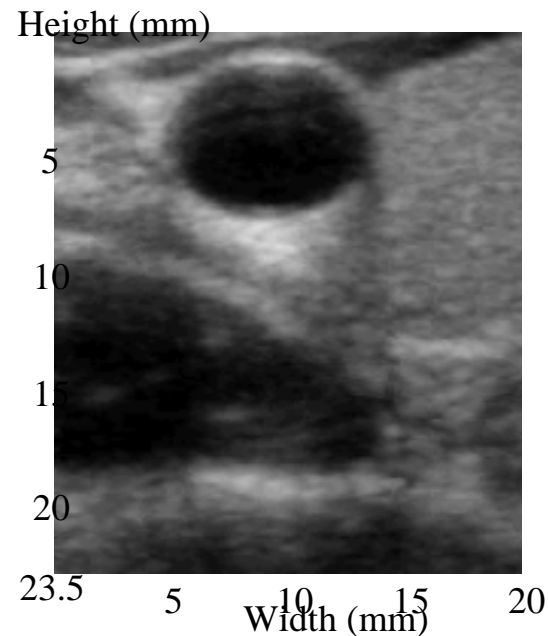
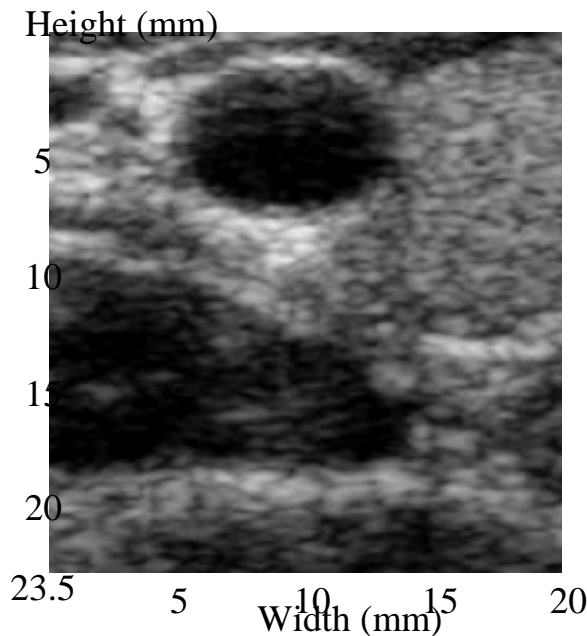
Cont'd

Thyroid

SNR=0.9625

SNR ↑

Computing speed ↑



L: original image

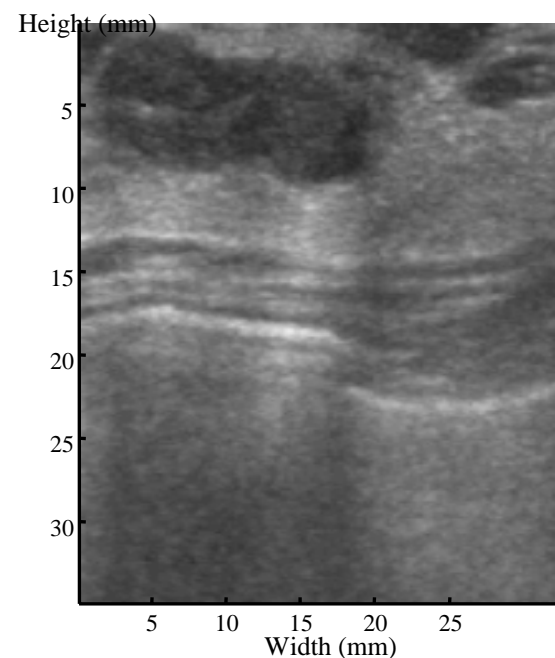
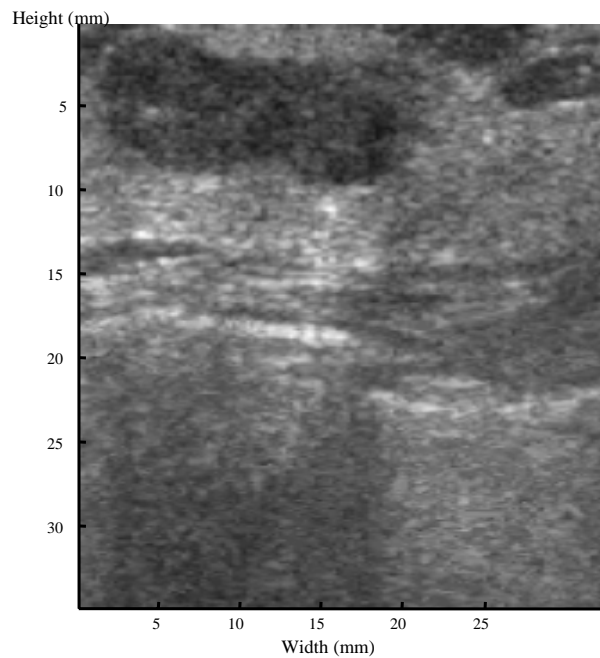
R: compounded image with BSP & Multilevel

Breast

SNR=0.1692

SNR ↑

Computing speed ↑

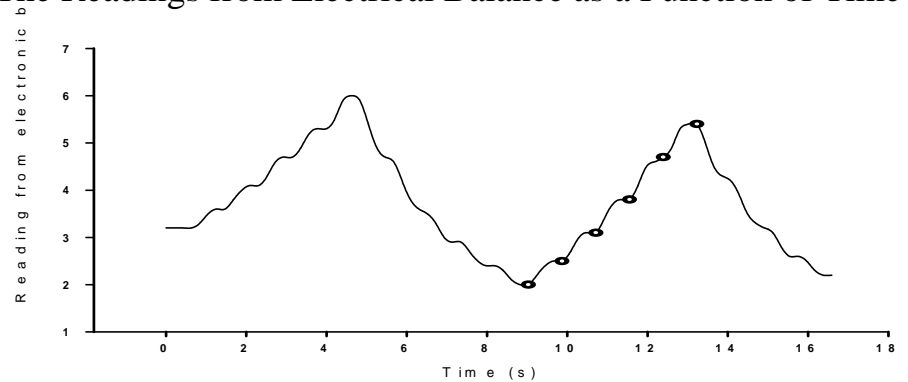


Young's Modulus Measurements of Human Liver and Correlation with Pathological Findings

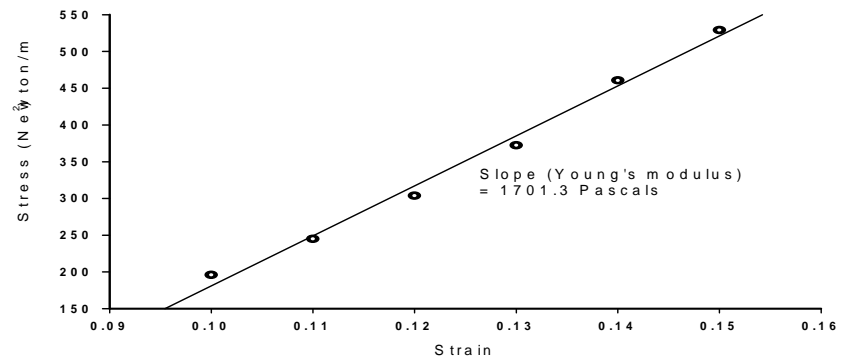
The Experimental Set-up



The Readings from Electrical Balance as a Function of Time



The Stress- Strain Curve

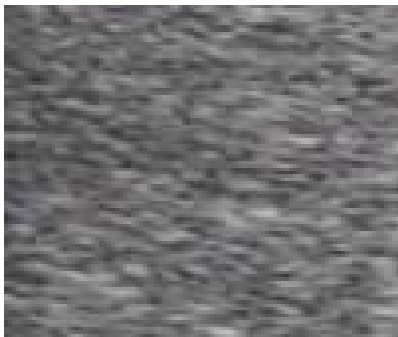


The Young's modulus of normal liver, cirrhotic liver and hepatic tumors

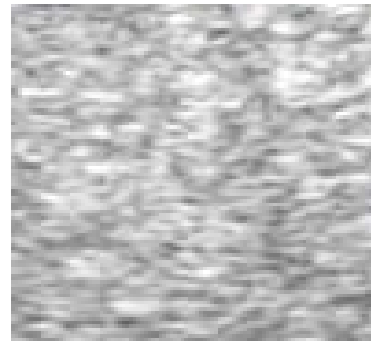
Preload strain	Young's Modulus (Pascals)						
	Liver parenchyma (mean value)			Hepatic tumors			
	Normal	Cirrhosis (Fibrosis score: 4)	Cirrhosis (Fibrosis score: 5)	Hepatocellular carcinoma	Cholangio-carcinoma	Focal nodular hyperplasia	Hemangioma (Emelianov et al. 1998)
5%	642.6	1106.4	1649.0	Smaller than normal liver	3003.7	1084.9	Larger than normal liver
10%	1083.6	2373.6	4930.7		12098.1	2522.5	

Tissue characterization of Ultrasonic B-image

- Compare normal with cirrhotic liver
 - Statistical method
 - Conventional and non-separable wavelet decomposition method



Normal liver

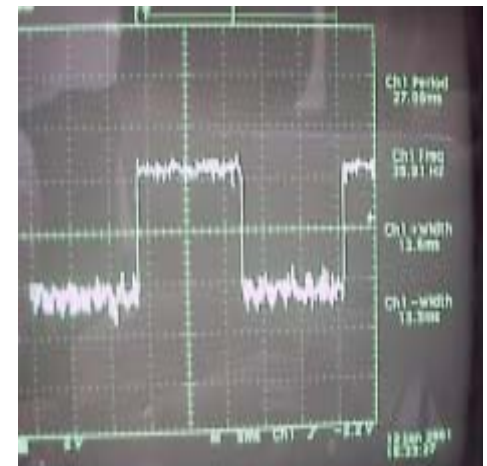


Cirrhotic liver

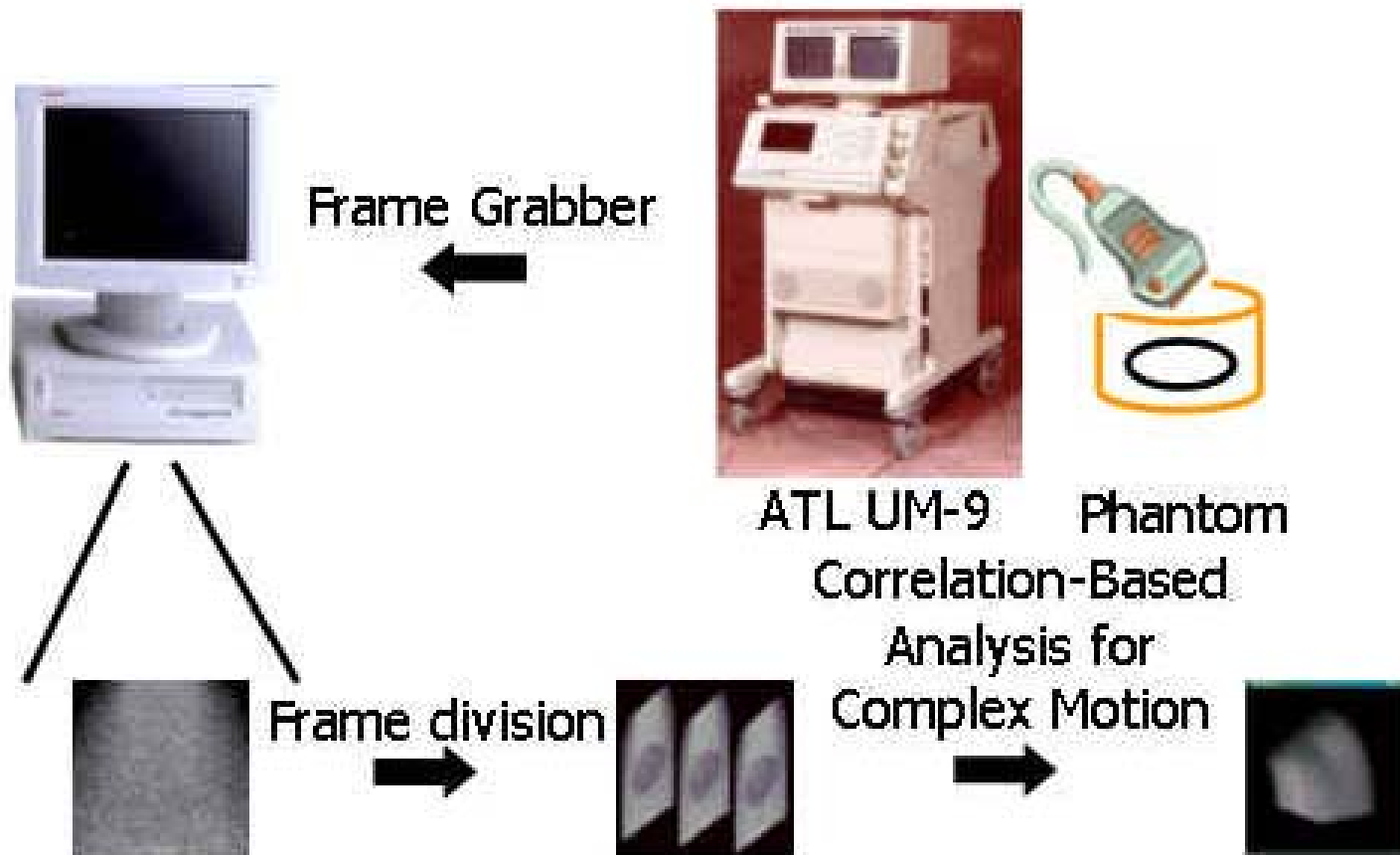
4. 3-D Ultrasound Imaging

Gyro Angle Detector for 3D Ultrasound

- **Hardware:**
 - **PG-03 Piezo GYRO(GWS)**
 - **8254 for counting pulse width**
 - **8051 with RS232 interface**
 - **IBM compatible PC**
- **Software:**
 - **Visual BASIC**



A Free-Hand 3D Ultrasound Imaging System



Correlation-Based Analysis for Complex Motion

Acquire 2 images

↓ Speckle tracking

Find x' , z' and y'

↓ Correct the x' and z' motions

Images are spatially matched

↓

Calculate 2D C.C.

↓ Go through all x', y', z' combinations

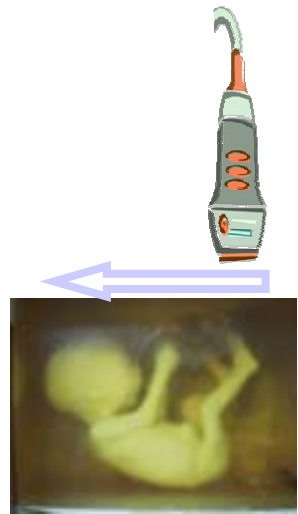
Find the best matched combination

↓

$x', y', z', \theta, \phi, \psi$

A 3D System Integration

- Platform :
 - Win NT、OpenGL

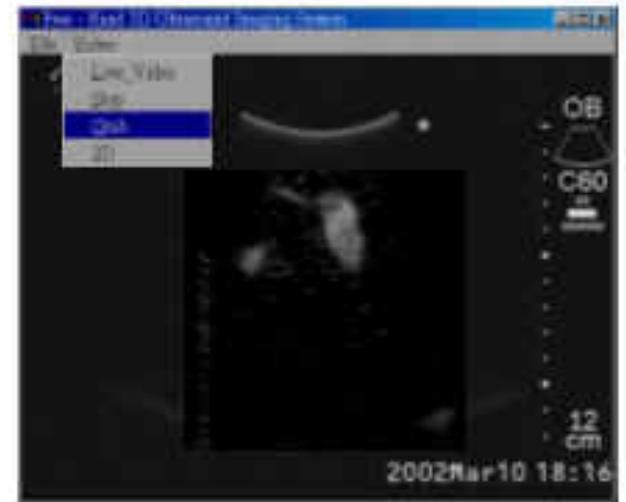


Baby Phantom



ATL UM-9

Frame Grabber
⇒



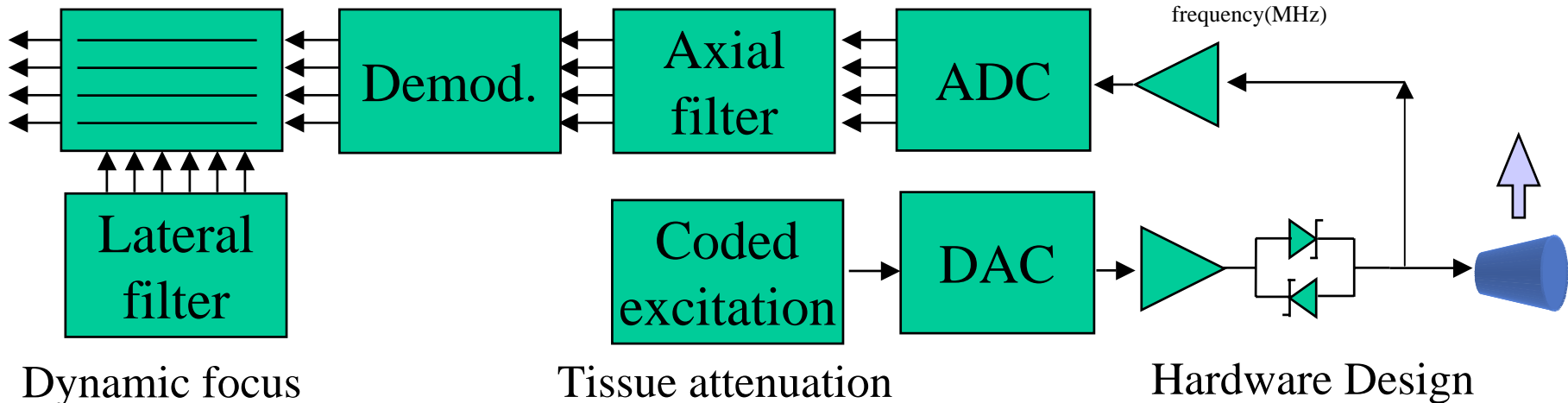
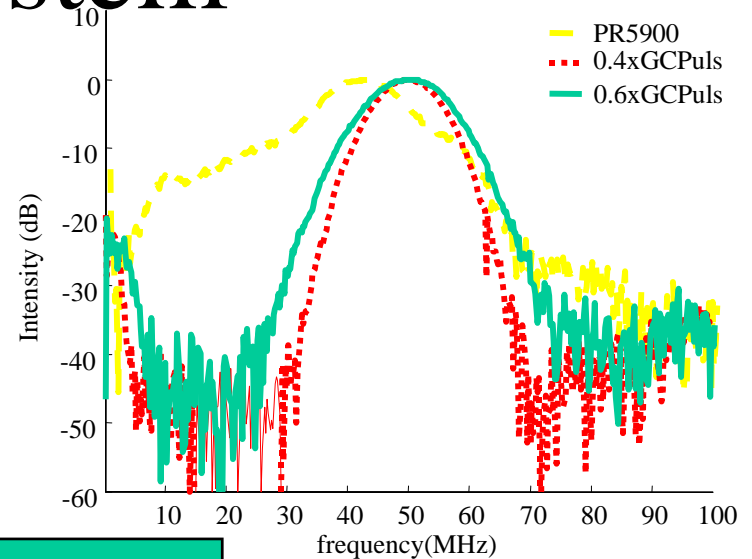
3D Rendering
⇒



5. High Frequency Ultrasonic Imaging

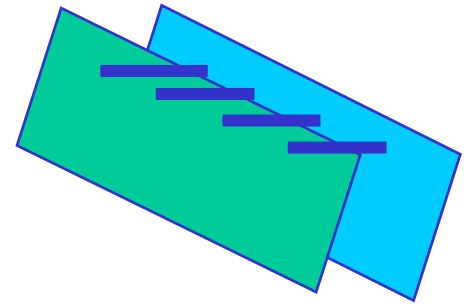
High frequency ultrasonic imaging system

- Fully digital system architecture
- 50 MHz center frequency
- 60 % fractional bandwidth



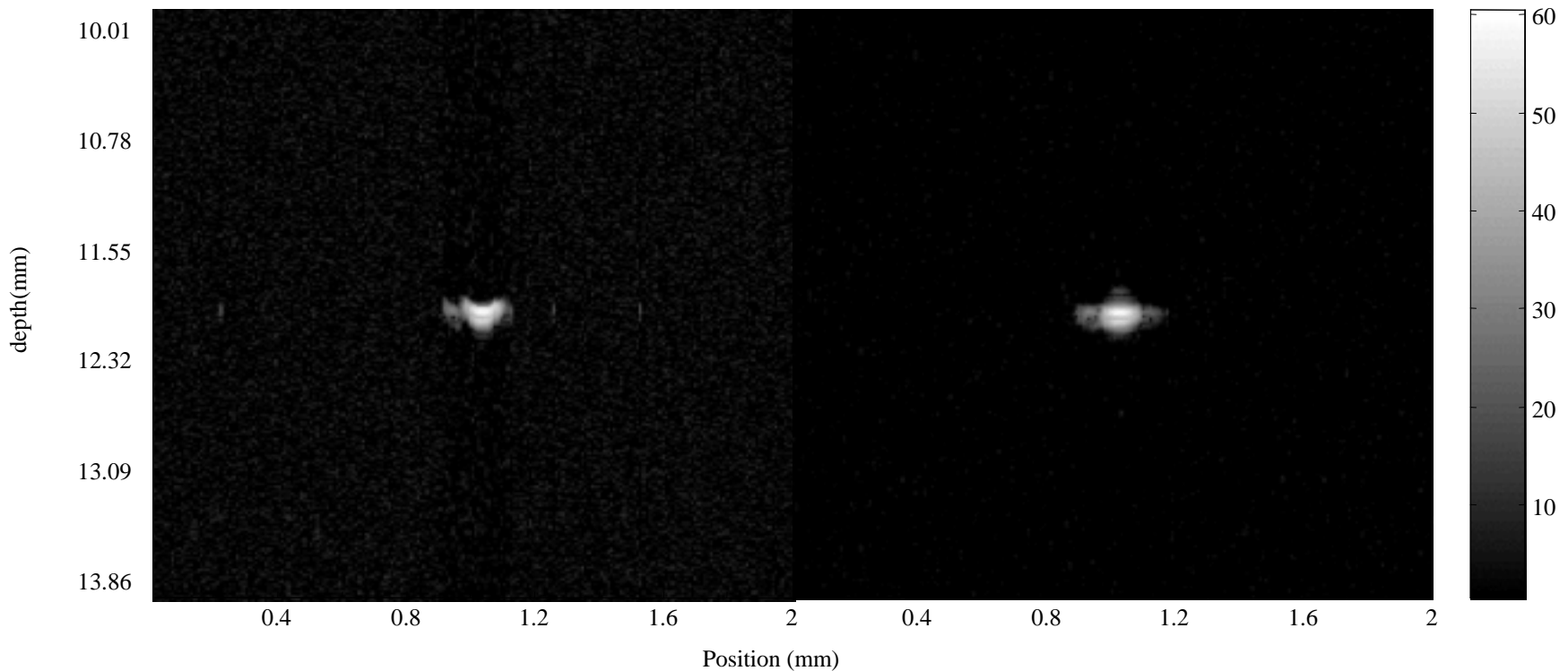
Wire phantom

Diameter = $52\mu\text{m}$ 



- 52um nylon wire phantom
- Gaussian Pulse

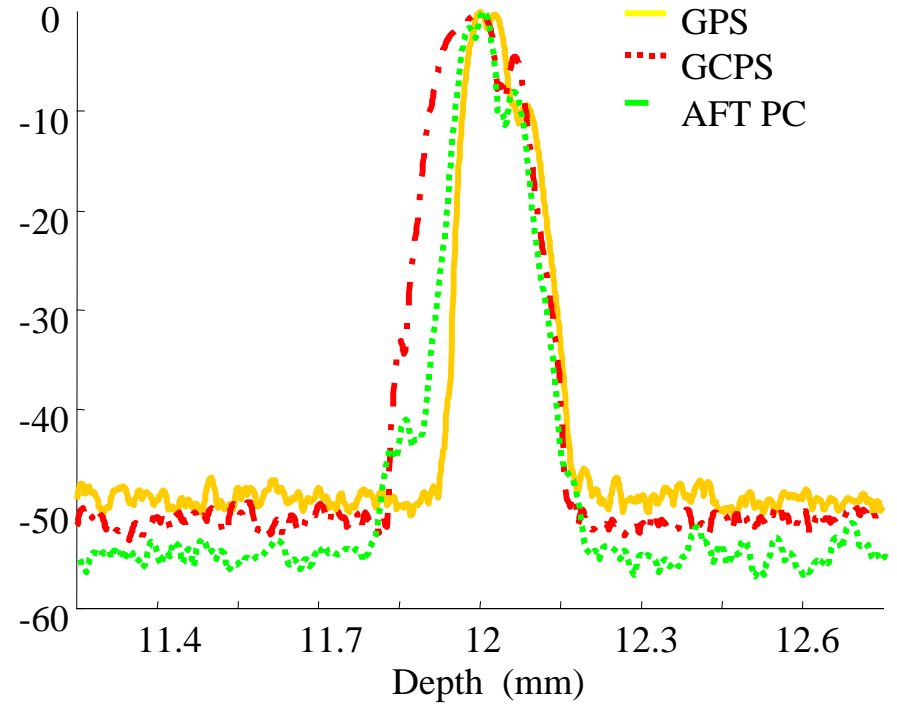
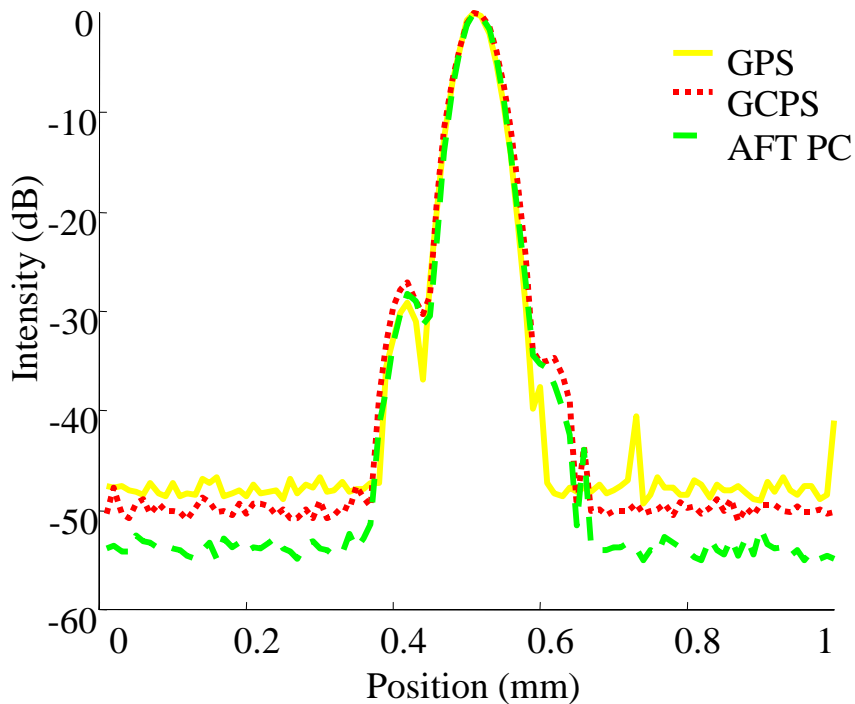
Gaussian Chirp Pulse



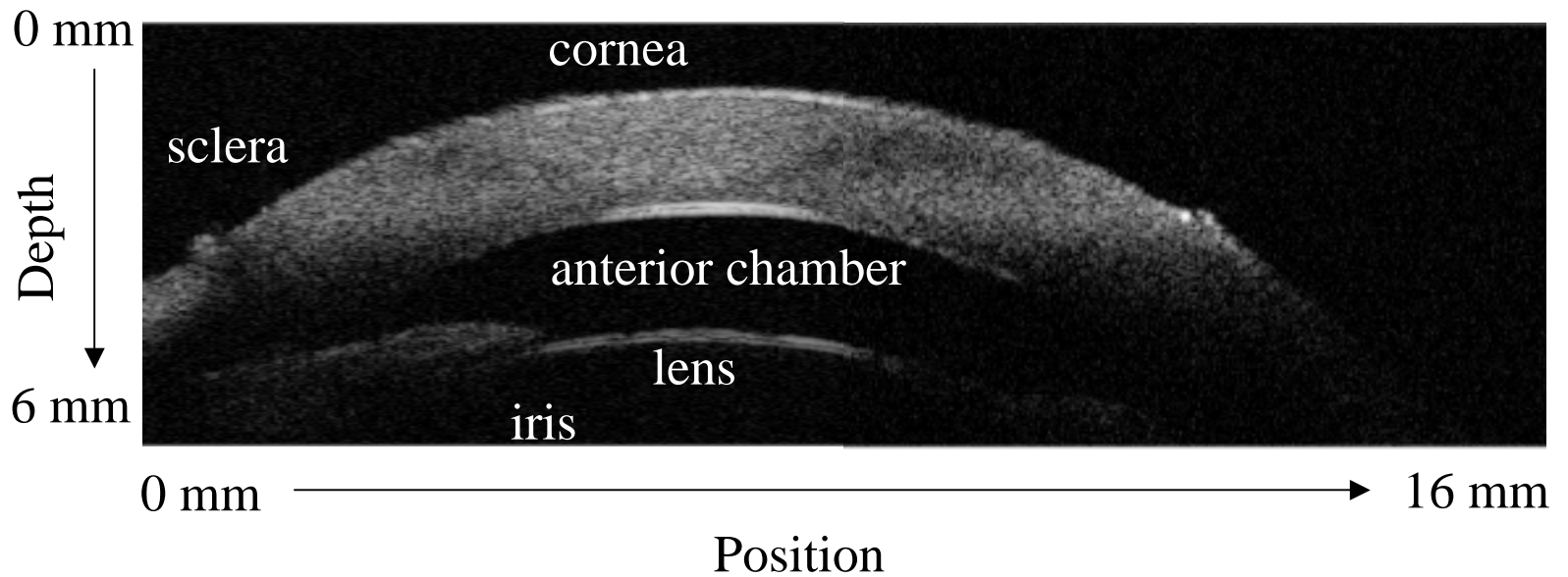
Resolution test

- Lateral projection:
- Spatial resolution is about $60\ \mu\text{m}$

axial projection

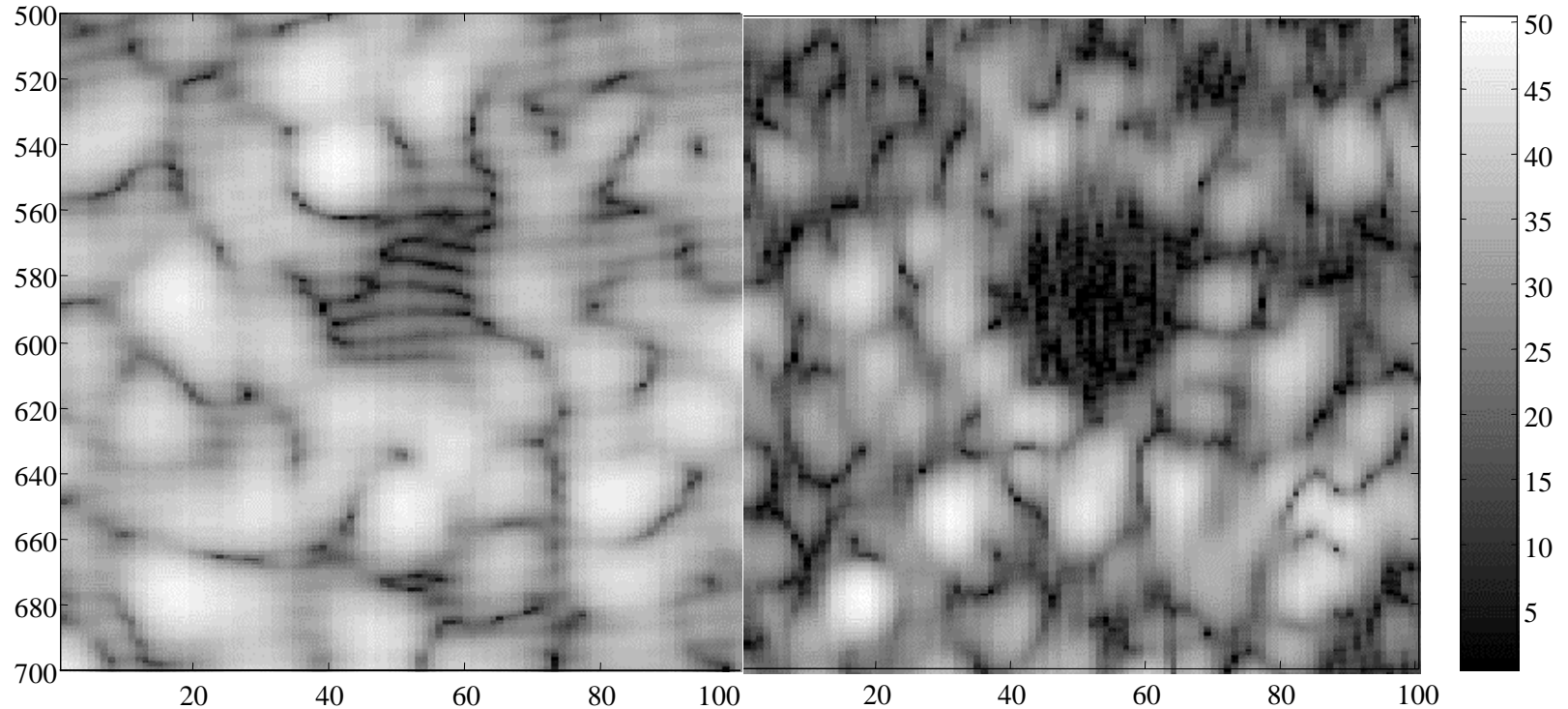


in-vitro pig eye image



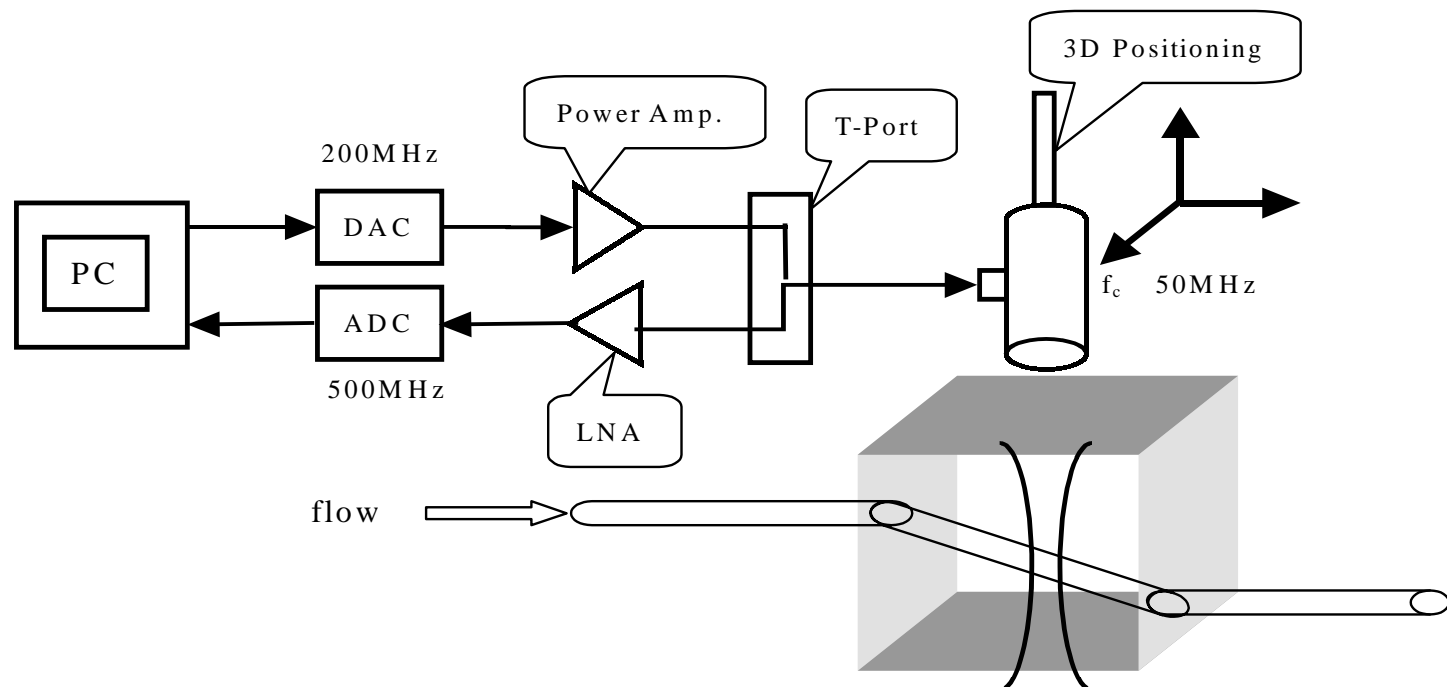
Tissue harmonic imaging

- Pulse inversion technique cancels fundamental signal



High Frequency Ultrasound Doppler

- 50MHz High Frequency Ultrasound : wideband transmitted signal (short transmitted pulse) and narrow lateral beamwidth better spatial and velocity resolution (down to mm/s), capable of estimating low velocities blood flow in small vessels.

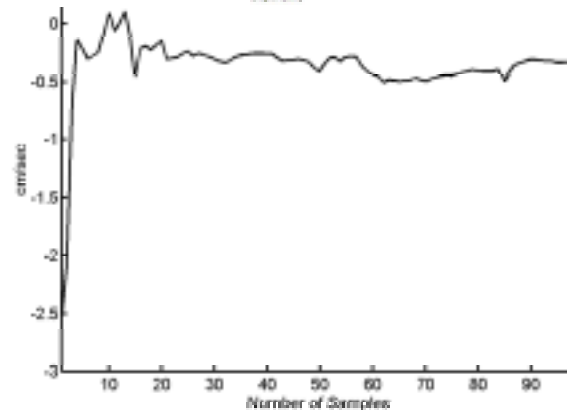
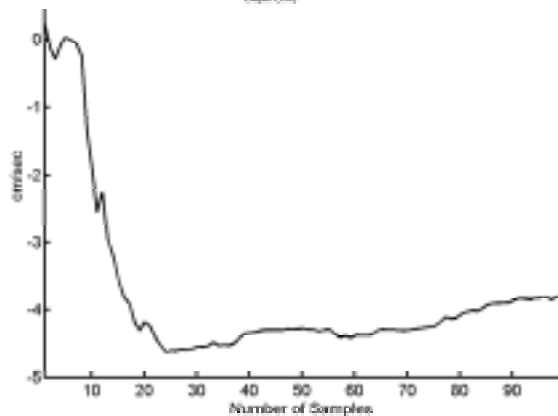
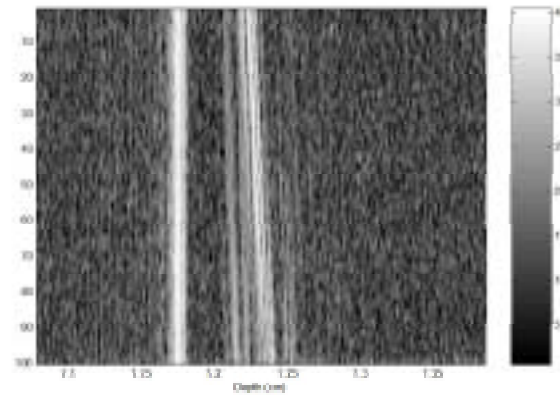
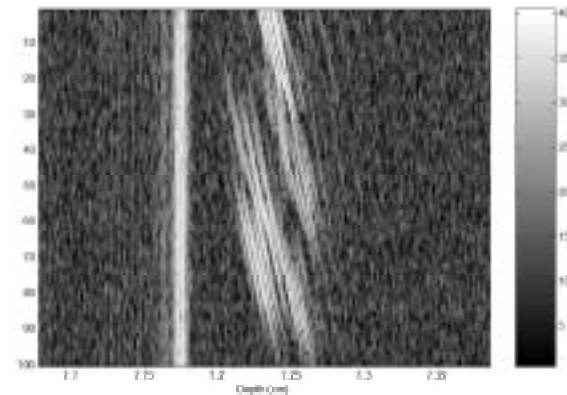


High Frequency Ultrasound Doppler

In-Vitro Flow Estimation : Autocorrelation Technique

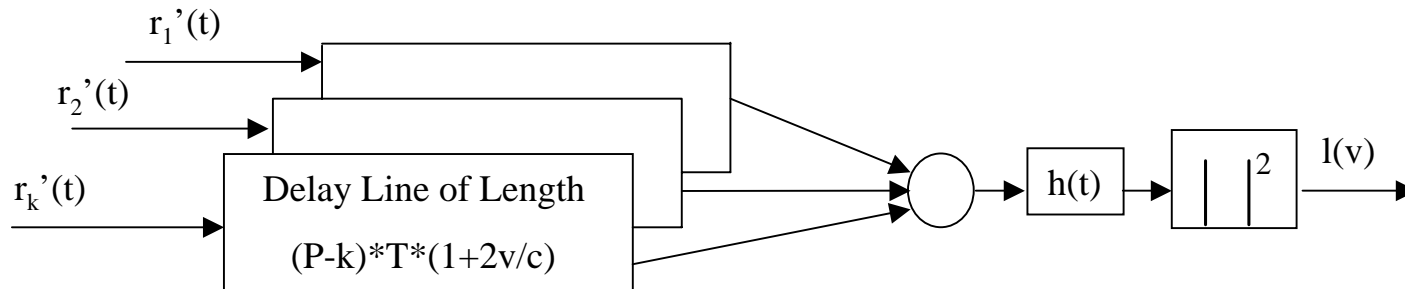
$$R(t) \equiv \int_{-\infty}^{\infty} S(t+\tau) S^*(\tau) d\tau$$

$$R(t) = |R(t)| e^{j\theta(t)} \longrightarrow \bar{f} = \frac{\theta(T)}{2\pi T}, \quad T : \text{PRI}$$

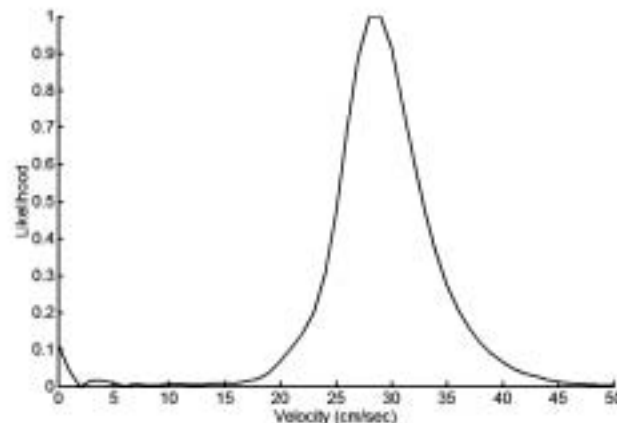


High Frequency Ultrasound Doppler

In-Vitro Flow Estimation : WMLE Technique

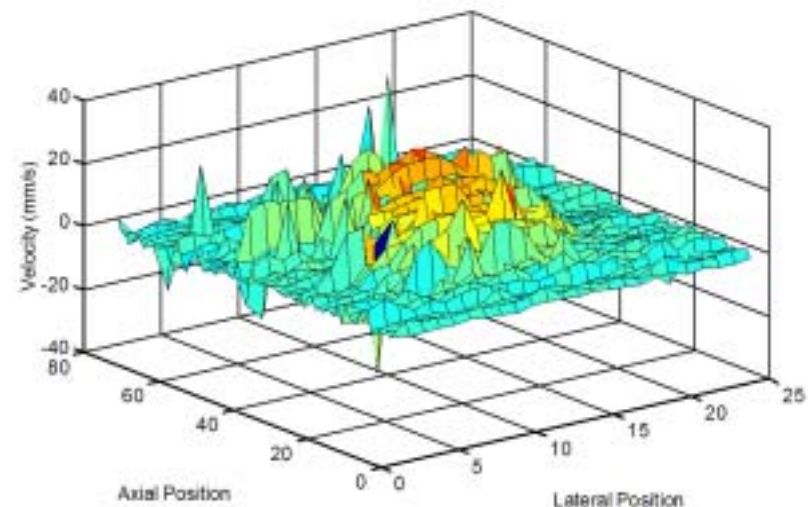
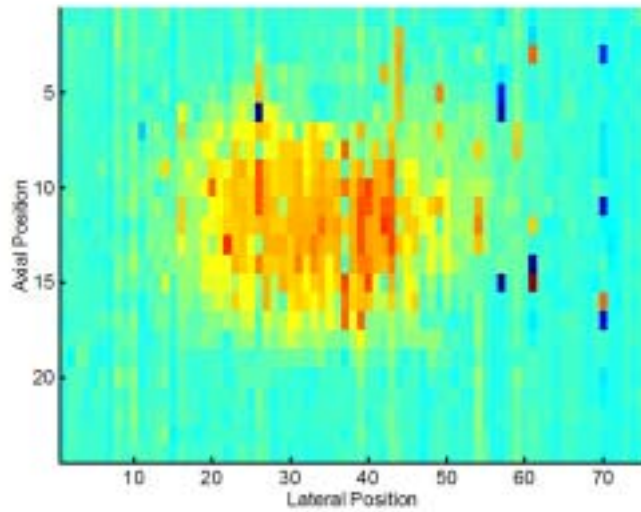
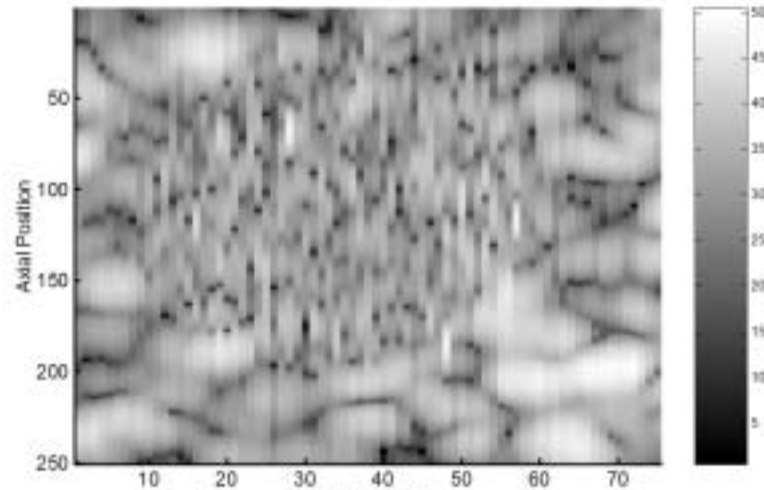


Bank of delay lines, and filter $h(t)$ matched to the expected demodulated echo signals which correspond to various velocities. The maximum likelihood velocity is then given by the filter with the largest output.



High Frequency Ultrasound Doppler

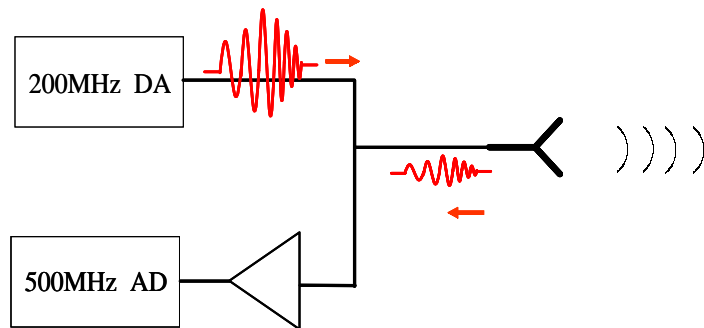
In-Vitro 2D Flow Data : 500 μ m diameter cyst,
with maximum velocity 20mm/s



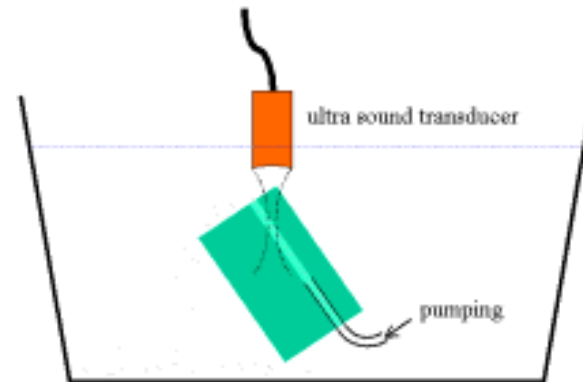
High Frequency Ultrasound Experiment

25~50MHz

Basic System Diagram



Flow System



Experiment Condition

200MHz DA excite 25~50 MHz coded ultrasound wave

500MHz AD receiving

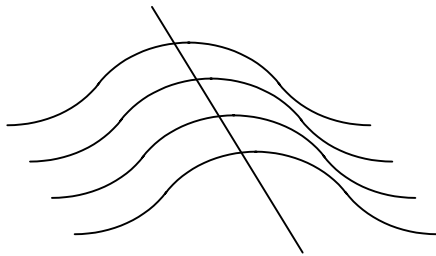
Wide band ultrasound transducer

Up to 20KHz PRF

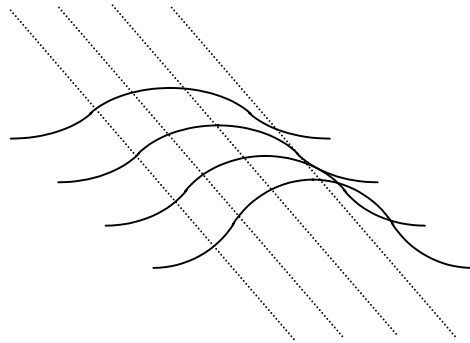
High Frequency Flow Estimation

RF Butterfly Search (Multi-line)

Traditional Butterfly Search Line

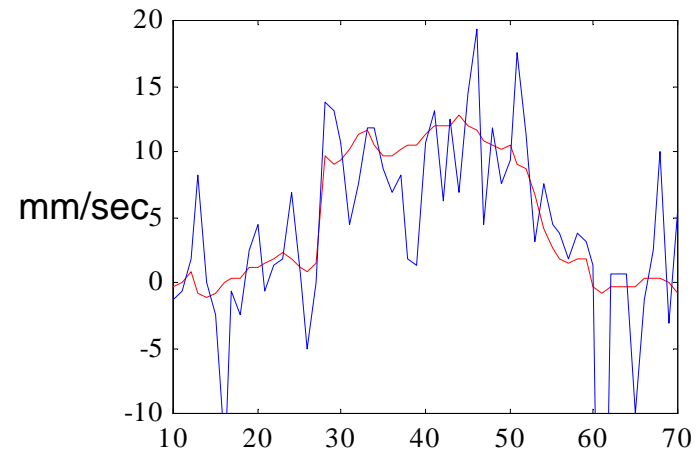


Multiple Butterfly Search Lines



Experimental -Flow Result

λ

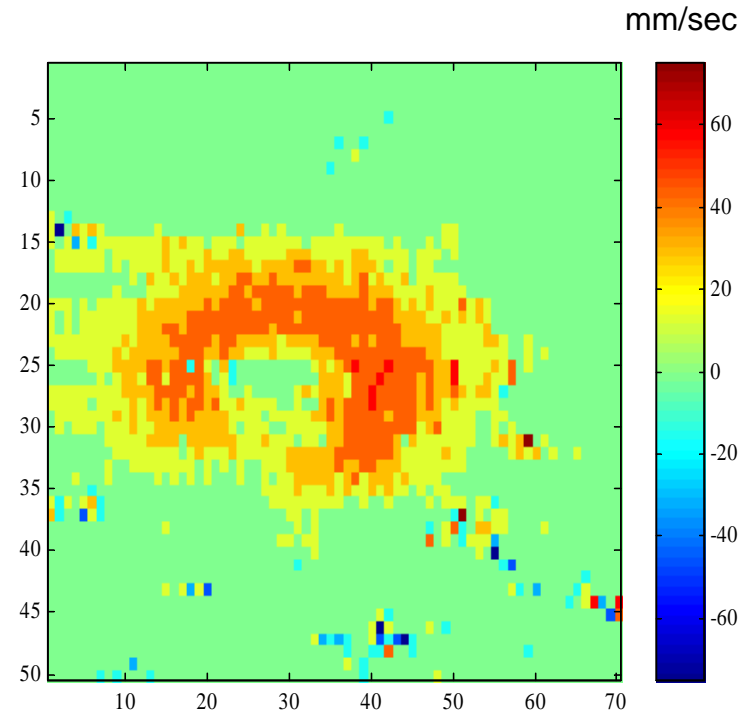
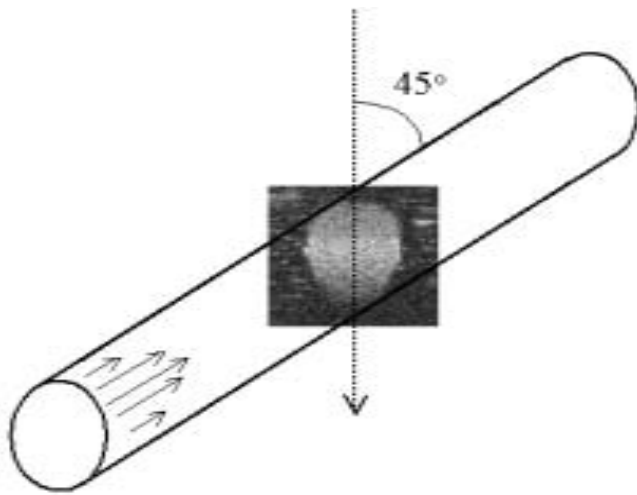


Traditional RF Butterfly 

Multi-line Butterfly 

High Frequency Flow Estimation

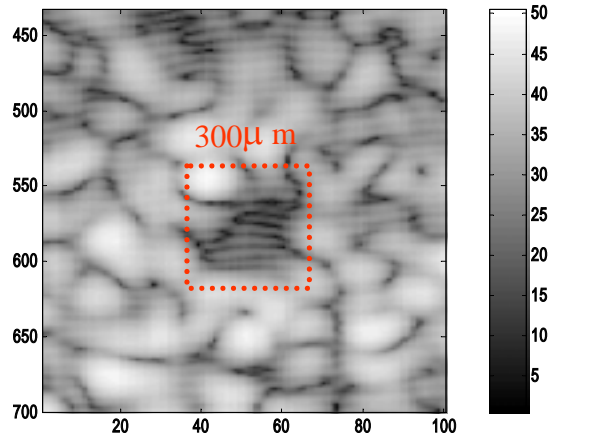
Color Flow Image



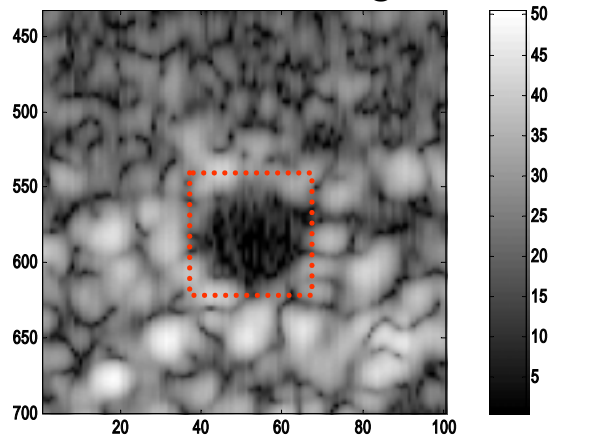
High Frequency Harmonic Image

25MHz 300 μ m Cyst image

Fundamental Image

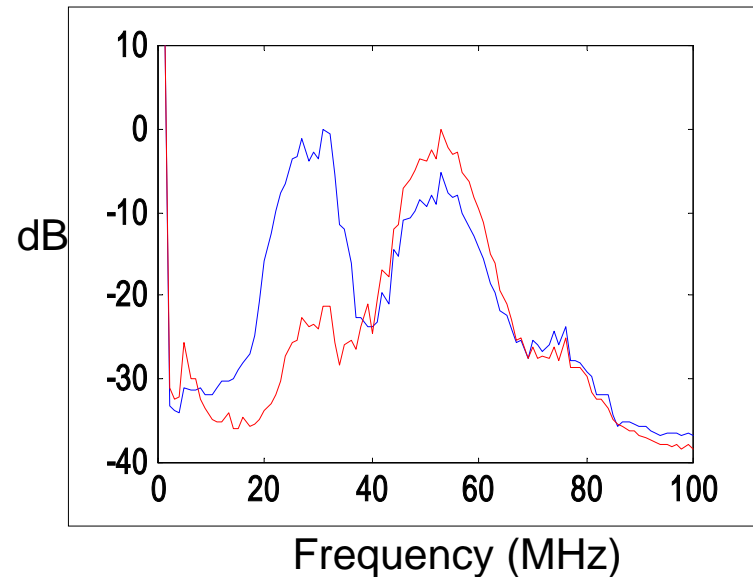


Harmonic Image



Fundamental Image ————

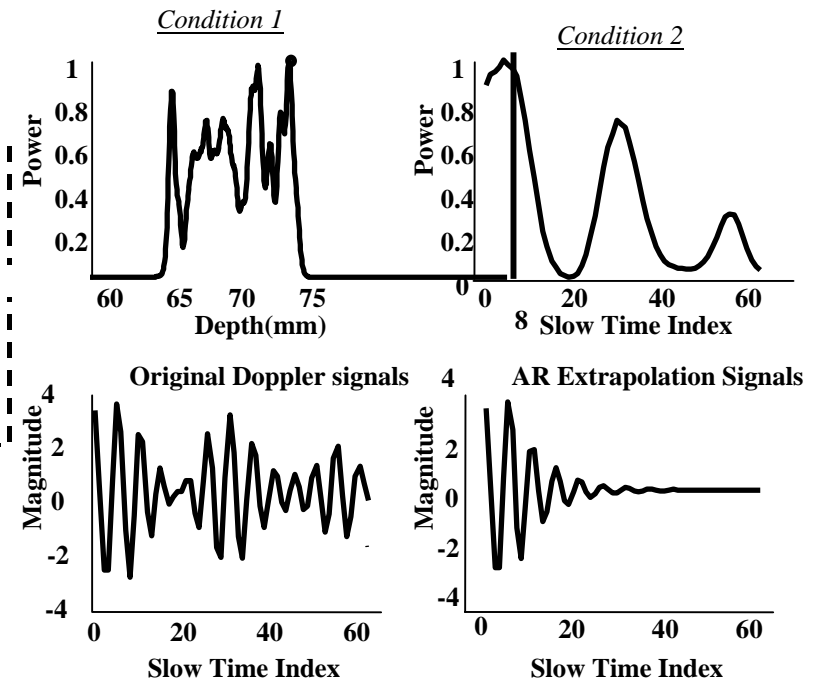
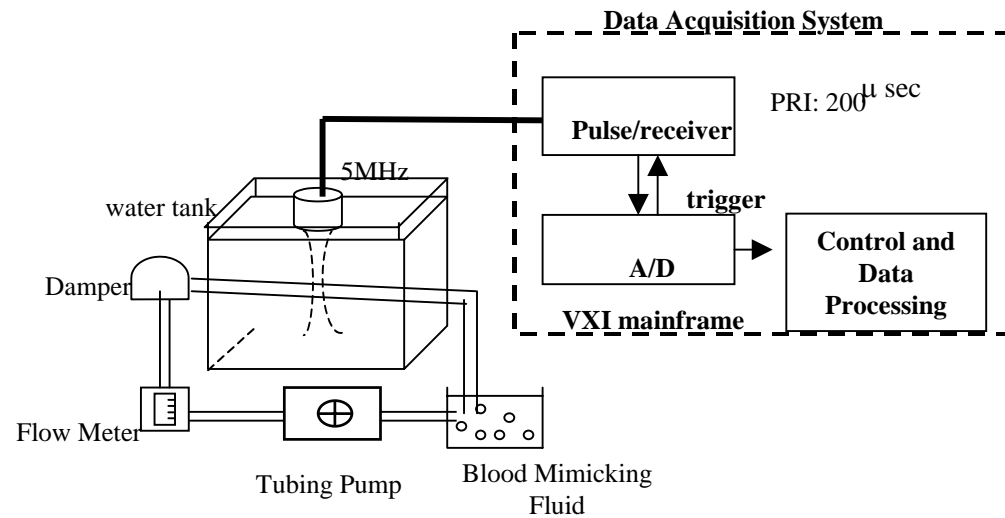
Harmonic Image ————



6. Blood Flow Estimation Using Ultrasonic Contrast Agent

Doppler Blood Flow Estimation (I)

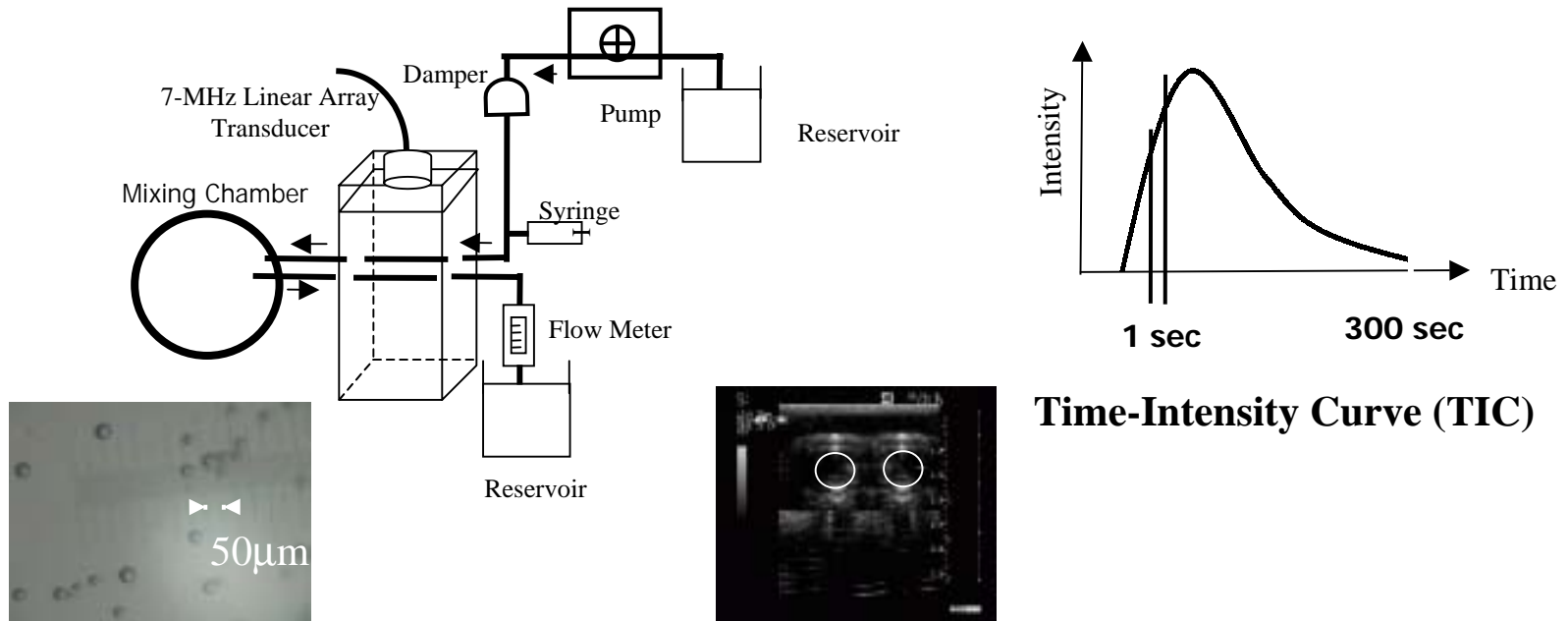
- Doppler Angle Estimation
- Blood Flow Estimation



1. P.-C. Li, C.-J. Cheng and C.-C. Shen, "Doppler Angle Estimation Using Correlation", IEEE Transactions on Ultrasonics, Ferroelectrics and Frequency Control, Vol. 47, No. 1, pp. 188-196, 2000.
2. P.-C. Li, C.-J. Cheng and C.-K Yeh, "On the Velocity Estimation Using Speckle Decorrelation", IEEE Transactions on Ultrasonics, Ferroelectrics and Frequency Control, Vol. 48, No. 4, pp. 1084-1091, July, 2001.
3. C.-K. Yeh and P.-C. Li, "Doppler Angle Estimation Using AR Modeling", IEEE Transactions on Ultrasonics, Ferroelectrics and Frequency Control. June, 2002

Blood Flow Estimation Using Ultrasonic Contrast Agent

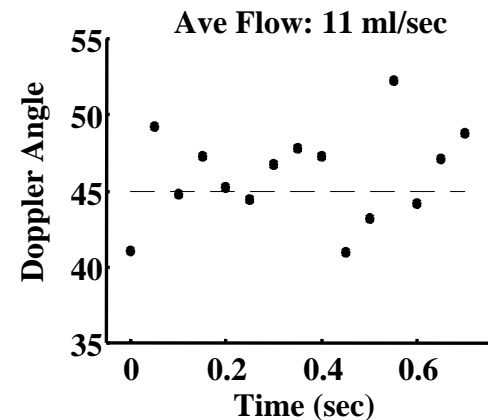
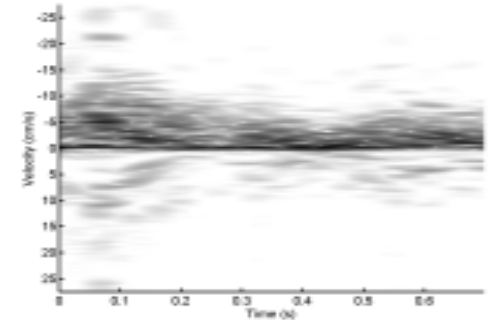
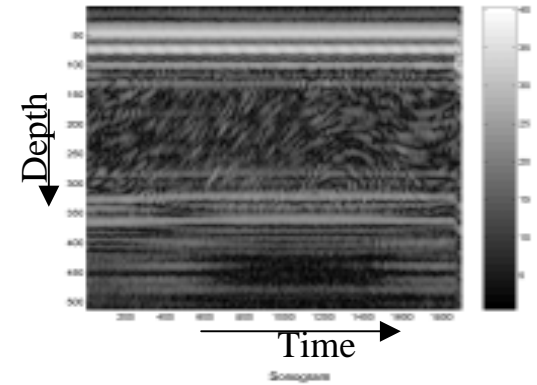
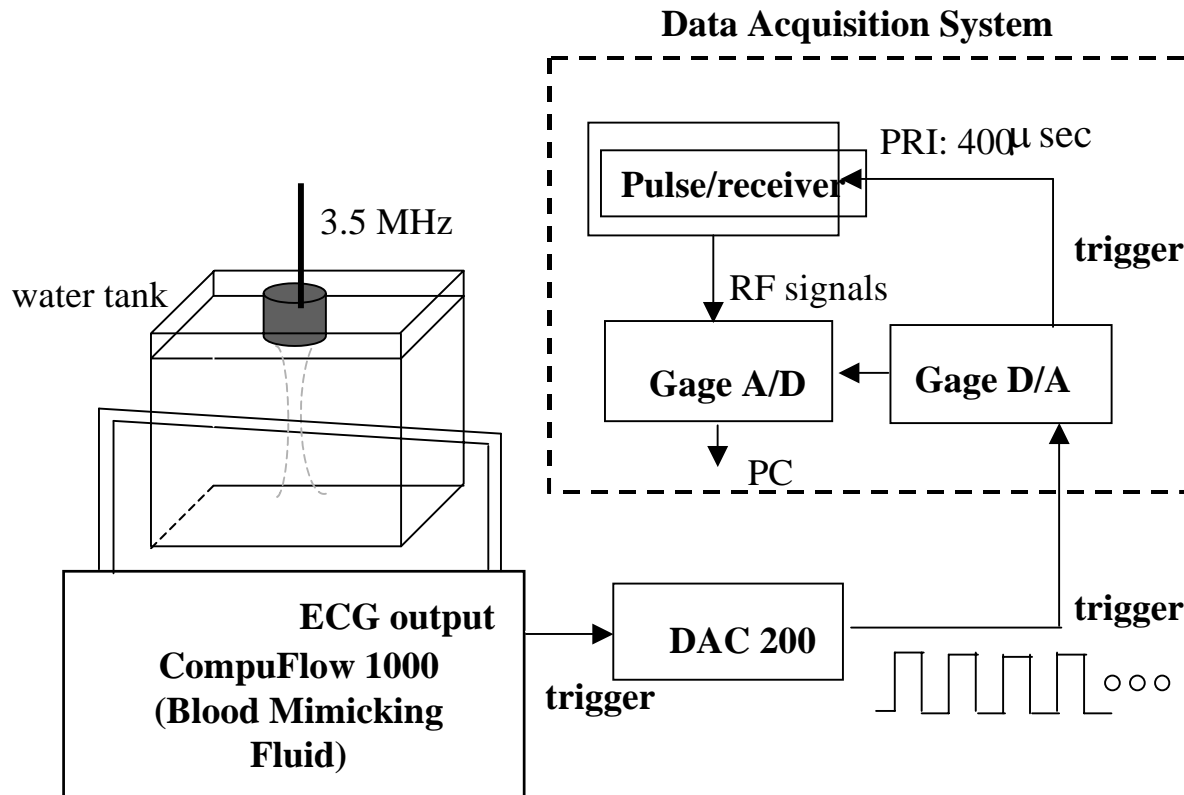
- Blood Flow Estimation (Indicator-Dilution Theory)
- Time-Vary Method



1. C.-K. Yeh S.-W. Wang and P.-C. Li, Feasibility Study on the Time-Intensity Based Blood Flow Measurements Using Deconvolution," *Ultrasonic Imaging*, vol. 23, pp. 90-105, April, 2001,
2. P.-C. Li, C.-K. Yeh and S.-W. Wang, "Time-Intensity Based Volumetric Flow Measurements: An In Vitro Study", *Ultrasound in Medicine and Biology*. vol. 28, no. 3, pp. 349-358, 2002

Doppler Blood Flow Estimation in Pulsatile Flow (II)

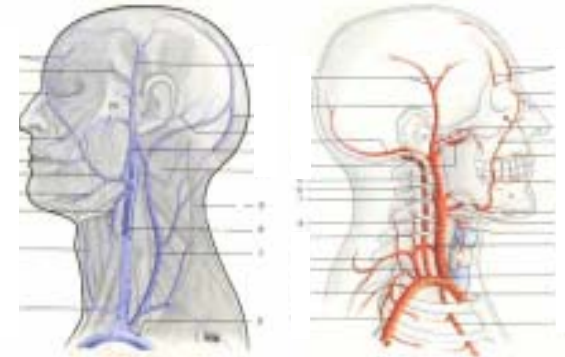
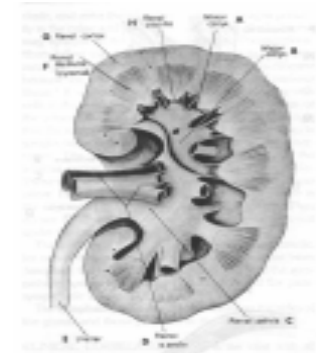
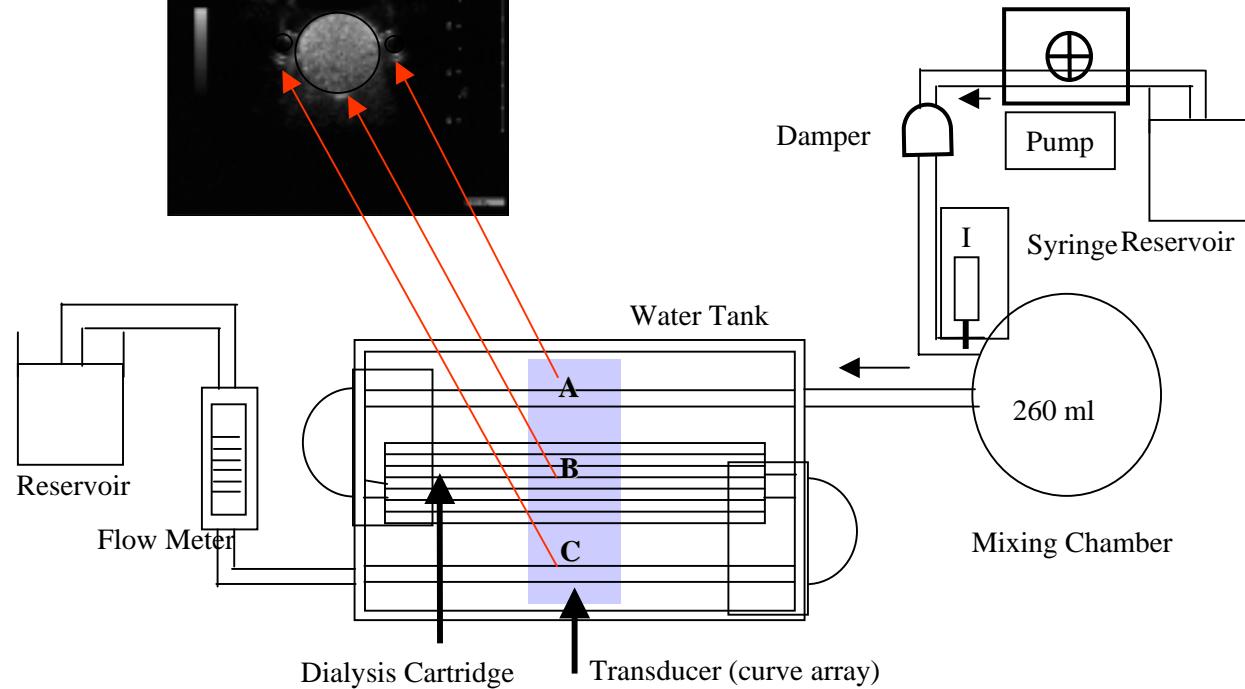
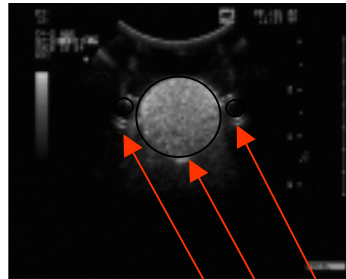
- Doppler Angle Estimation
- Blood Flow Estimation



1. Chih-Kuang Yeh and P. C. Li, "Doppler Angle Estimation of Pulsatile Flow Using AR Modeling," *Ultrasonic Imaging*, 2002 (submitted)

Blood Flow Estimation Using Ultrasonic Contrast Agent

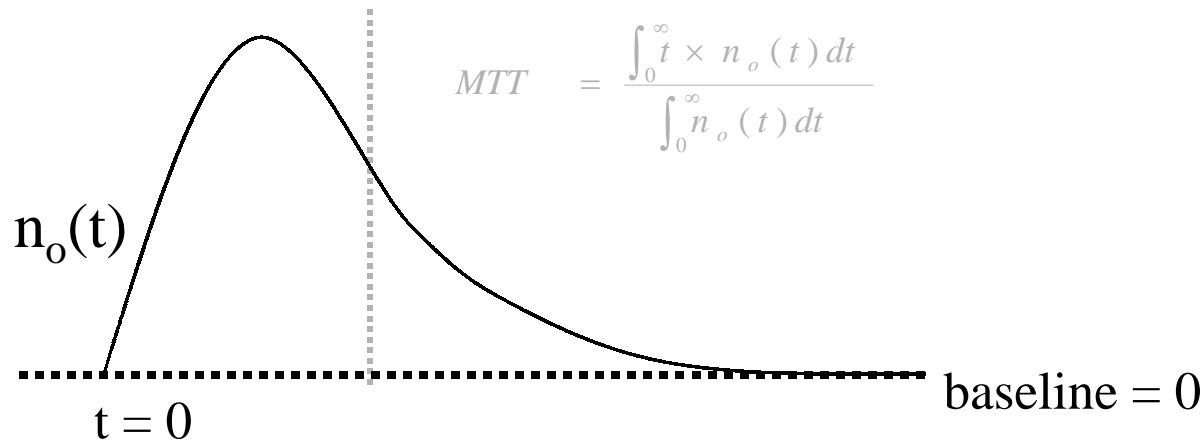
- Shadowing Effect
- Input and Output Time-Intensity Curves (IOTIC)



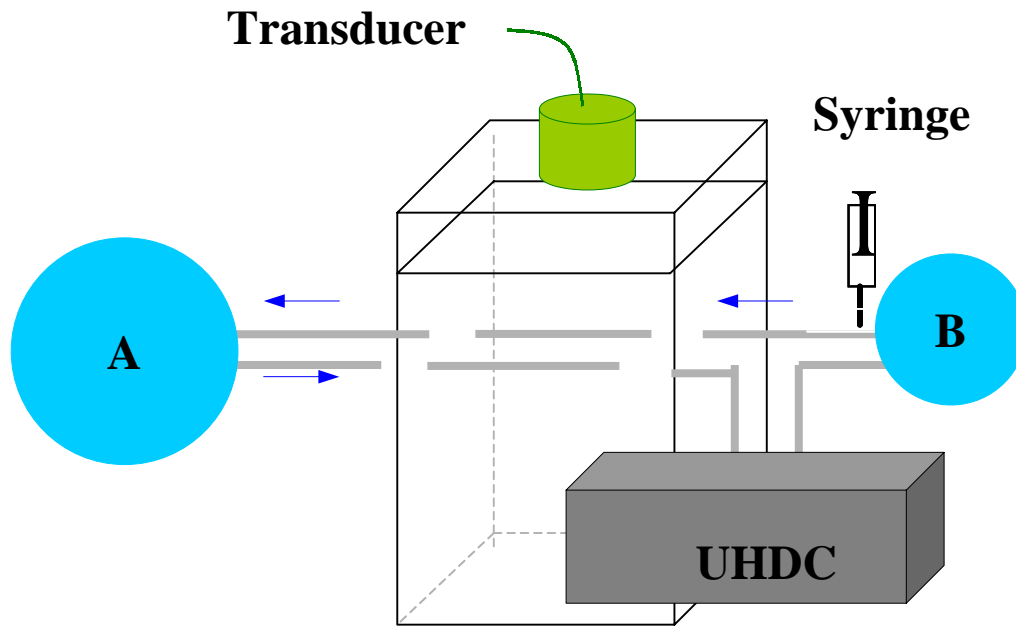
1. Chih-Kuang Yeh and P. C. Li, "Contrast specific ultrasonic flow measurements based on both input and output time intensities," *Ultrasound in Medical & Biology*, 2002 (Submitted)

Assessment of Parameters in Pulsatile Flow using Ultrasound Contrast Agent

- Provide a model for the assessment of perfusion characteristics
- Dilution theory
 - MTT : mean transient time
 - theory : V/Q (ideal)
- LTI system \longrightarrow TV (time-varying)



Experimental setup

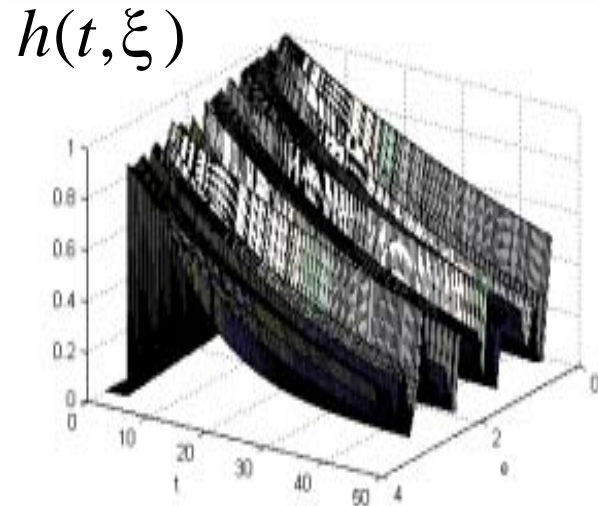
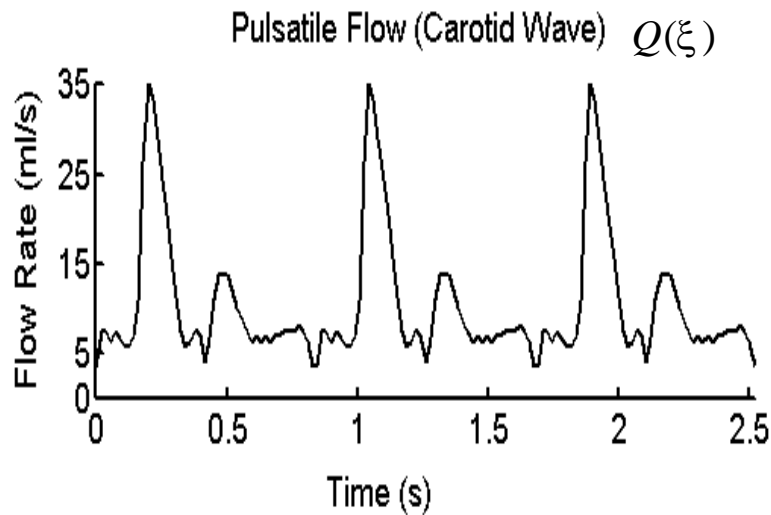


Simulation methods

Superposition theory :

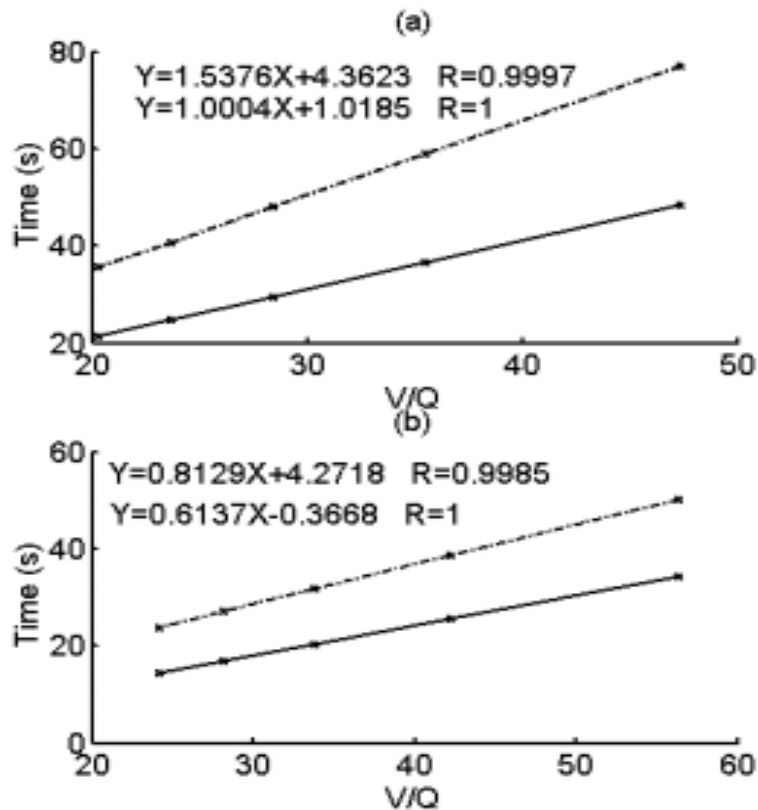
$$I_o(t) = \int_{-\infty}^{\infty} h(t, \xi) I_I(\xi) d\xi$$

$$h(t, \xi) = \begin{cases} 0 & t < \xi \\ e^{-Q(\xi)t/V} & t \geq \xi \end{cases}$$

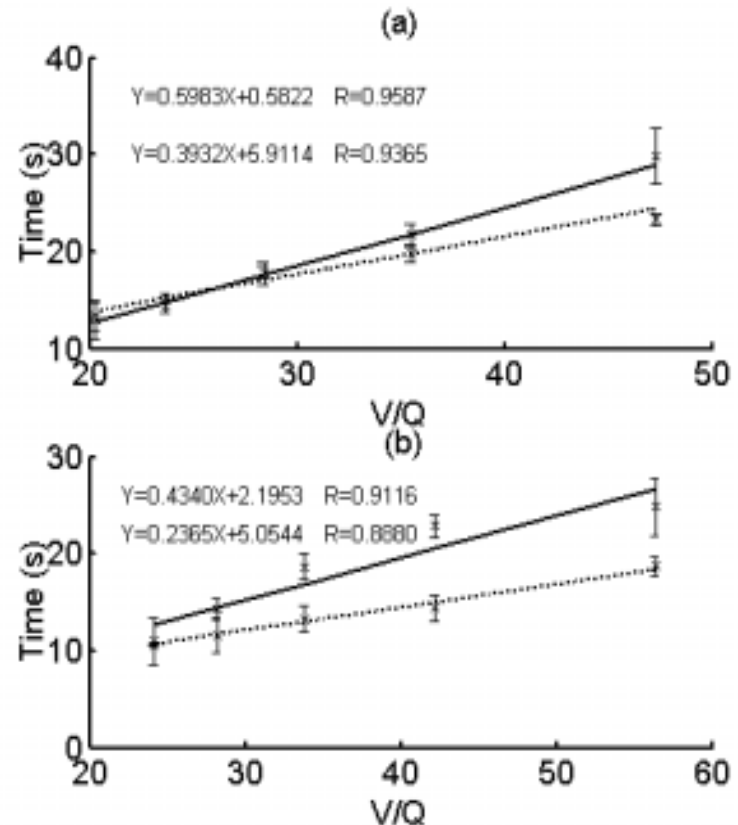


Results: the theoretical values & MTT

simulation result



experimental result



EQUIPMENT (1)



Panametrics Model 5900 PR (pulser / receiver)	1	200 MHz digital
GW Model GFG-813 (function generator)	1	
GW Model GFG-8016D (function generator)	1	
HP Model 54603B (oscilloscope)	1	60 MHz 附 probe X 4 power line X 1
Tektronix Model TDS 380 (oscilloscope)	1	Two channel / digital real-time / 400MHz / 2GS/s
TAIK Model TK-12001D (DC power supply)	1	
EPE Model EP-3000 (DC power supply)	1	
Cimarec Model SP46925 (stirrer/heater)	1	S/N:1069980822742
OHAUS Model IP12KS	1	
Microtime Model 51/52-E (WINICE)	1	S/N:A00I955172
Cole Parmer Model 07596-20 (damper)	1	
Cole Parmer Model 77021-60 (pumper)	1	
GaGe Model CompuGen 1100 (AFG)	1	ISA interface 1M RAM on board S/N: G00086 80 MHz
GaGe Model CompuScpoe 12100 (A/D)	1	PCI interface 1M RAM on board S/N: P10243 100 MHz
Amplifier Research LN1000A(LNA)	1	DC transformer
Amplifier Research P25A250A(PA)	1	
Signatec DAC200	1	User manual , CDX1,BNC to SMD cableX3
Signatec PDA500	1	User manual , CDX1
Signatec PMP8-A	1	User manual , CDX1
Panametrics HF cable	3	1 ft., 3 ft., 6ft.

EQUIPMENT (2): Transducer



EQUIPMENT (3): Commercial Ultrasound Machine



(SonoSite)
(hand-carried ultrasound system)



(ATL Ultramark 9 HDI)

EQUIPMENT (4): Phantom



Breast (I)

Breast (II)

Baby

EQUIPMENT (5)



(Digital Sonifier, BRANSON)
Making Microbubbles



(UHDC Flow System)
Simulation Physical Pulsatile Flow